ESD-TR-74-304

MTR-2851

CLUTTER SUPPRESSION BY MEANS OF DIGITAL MTI
AS APPLIED TO PRECISION APPROACH RADAR

R. J. Long

DECEMBER 1974

Prepared for

DEPUTY FOR PLANNING, TECHNOLOGY, AND REQUIREMENTS
ELECTRONIC SYSTEMS DIVISION
AIR FORCE SYSTEMS COMMAND
UNITED STATES AIR FORCE
L. G. Hanscom Field, Bedford, Massachusetts

ADA004475

REVIEW AND APPROVAL

This technical report has been reviewed and is approved for publication.

John F Donegan

JOHN R. DONEGAN
Project Engineer

FOR THE COMMANDER

Joseph L Masi

JOSEPH L. MASI, Colonel, USAF
Director, Technology
Deputy for Planning, Technology
 and Requirements

REPORT DOCUMENTATION PAGE		READ INSTRUCTIONS BEFORE COMPLETING FORM
1. REPORT NUMBER ESD-TR-74-304	**2. GOVT ACCESSION NO.**	**3. RECIPIENT'S CATALOG NUMBER**
4. TITLE *(and Subtitle)* CLUTTER SUPPRESSION BY MEANS OF DIGITAL MTI AS APPLIED TO PRESICION APPROACH RADAR		**5. TYPE OF REPORT & PERIOD COVERED**
		6. PERFORMING ORG. REPORT NUMBER MTR-2851
7. AUTHOR(s) R. J. Long		**8. CONTRACT OR GRANT NUMBER(s)** F19628-73-C-0001
9. PERFORMING ORGANIZATION NAME AND ADDRESS The MITRE Corporation Box 208 Bedford, Mass. 01730		**10. PROGRAM ELEMENT, PROJECT, TASK AREA & WORK UNIT NUMBERS** Project No. 7080
11. CONTROLLING OFFICE NAME AND ADDRESS Deputy for Planning, Technology, and Requirements Electronic Systems Division, A. F.S.C. L. G. Hanscom Field, Bedford, Mass. 01730		**12. REPORT DATE** DECEMBER 1974
		13. NUMBER OF PAGES 69
14. MONITORING AGENCY NAME & ADDRESS*(if different from Controlling Office)*		**15. SECURITY CLASS. *(of this report)*** UNCLASSIFIED
		15a. DECLASSIFICATION/DOWNGRADING SCHEDULE

16. DISTRIBUTION STATEMENT *(of this Report)*

Approved for public release; distribution unlimited.

17. DISTRIBUTION STATEMENT *(of the abstract entered in Block 20, if different from Report)*

18. SUPPLEMENTARY NOTES

19. KEY WORDS *(Continue on reverse side if necessary and identify by block number)*

RAIN CLUTTER MODEL
CLUTTER SUPPRESSION
FINITE IMPULSE RESPONSE DIGITAL FILTERS
DIGITAL FILTERS

20. ABSTRACT *(Continue on reverse side if necessary and identify by block number)*

A major concern in the design of X-Band precision approach radars is the detection and tracking of aircraft in heavy rain clutter. The objective of this investigation was to explore the ability of a particular digital band-pass filter to discriminate Doppler shifted aircraft from such clutter. The filter was designed and tested in software using complementary PRFs. Rain clutter was modeled statistically using realistic parameters. The range-azimuth-elevation cell size employed was 150 m. x 1° x 1°. A clutter-to-signal ratio of 20 db, corresponding to a 1 m^2 aircraft at 10 Km. in a rainfall of 50 mm/hr at

20. (Cont.)

10 GHz., was tested. The filter was characterized by n predetermined weights, $W_1, W_2, \ldots W_n$. The filtering operations consisted of multiplying the complex return in a given range cell on transmission 1 by W_1, transmission 2 by W_2, etc., then adding the results for n transmissions, and computing the magnitude. Results are given for n = 15, 19, and 23. The results for n = 15 were poor and for n = 19 were encouraging. A clutter suppression of 40 db. was obtained for n = 23 which is considered worthy of consideration for future system design.

TABLE OF CONTENTS

LIST OF ILLUSTRATIONS

LIST OF TABLES

GLOSSARY

$w(i)$ Filter Weights

$W(f)$ Response of Filter at Frequency f

λ Free Space Wavelength of Radar

PRF   Pulse Repetition Frequency

PRI   Pulse Repetition Interval

$R(\ell)$ ℓ^{th} Sampled Video (amplitude and phase)

A_K Amplitude of Kth Scatterer

V_K Radial Velocity of Kth Scatterer

$\sqrt{\sigma_T}$ Amplitude of Target

V_T Radial Velocity of Target

ϕ_K Initial phase of Kth Scatterer

F_i Output of Filter i (i = 1,6), @ 8.0 and 5.33 KHz respectively.

p Power of Returned Signal

A Square Root of Power of Returned Signal

$\rho_{II}(\tau)$ Auto-correlation of In-Phase (I) Channel

$\rho_{IQ}(\tau)$ Cross-correlation of In-Phase (I) Quadrature (Q) Channel

$\rho(\tau)$ Auto-correlation Function with Average Velocity Removed.

3

SECTION I

INTRODUCTION

The primary function of precision approach radars is the detection
and tracking of landing aircraft during final approach, oftentimes
in the presence of heavy rainfall clutter. Because the operation
of such radars has been restricted to X-Band and because the radar
cross section of rain is an increasing function of frequency, techniques
for discrimination of aircraft from rain clutter are of major concern
to the system design process. Available discrimination techniques
are (1) the use of circular polarization, (2) the use of high range
resolution, and (3) the use of Doppler resolution or MTI. For example,
the AN/TPN-19 PAR uses a combination of all three, each contributing
toward the whole. However, this design approach has proved costly.
Currently, the AN/GPN-XX PAR program is considering approaches of
lower cost potential.

In order to provide an enlarged technical data base applicable
to the AN/GPN-XX program, Project 7080 entitled Aircraft Detection
in Rain was conducted in Fiscal Year 1974 for the Electronic Systems
Division, USAF, by the MITRE Corporation. This project embraced three
specific tasks: (1) the experimental measurement of the depolarization
of circular polarization by rain at X-Band, (2) the investigation of
a linearly polarized, low cost, electronically scanned antenna, and
(3) the application of digital filtering techniques to the discrimination

4

of rain clutter through Doppler resolution of target and clutter.
As a result of a review of this project by the Rome Air Development
Center in its early stages, the application of effort applied to
the depolarization measurements was emphasized and that applied to
the antenna and digital filtering tasks was diminished.

This report presents the results of the digital filtering
application study. The results of the study of circular polarization
degradation are given in Reference 1 and those of the low cost antenna
study are given in Reference 2. The principal conclusions of this
report are that the suppression of rain clutter by 40 dB solely
through the application of digital filtering techniques appears
feasible and that its use in conjunction with the linearly polarized
low cost antenna approach of Reference 2 could possess significant
potential for a low cost system design. The degradation data of
Reference 1 on the other hand should be useful to system design
concepts which utilize circular polarization for suppression inasmuch
as very little data of this kind is available.

In this report digital filtering techniques are applied to
the specific goal of discriminating aircraft approaching at represent-
ative landing velocities from heavy rainfall clutter. This application
of digital filtering in effect constitutes a digital moving target
indicator in the sense that the output is not a replica of the input
signal, but rather a number related to its amplitude and frequency.
A separate digitized number of this type is provided for each

5

range resolution cell. The digital filtering provides a band-stop characteristic which severely attenuates the amplitude of fixed or slowly moving clutter and a band-pass characteristic which does not affect significantly the amplitude of targets moving at final approach velocities. A threshold can be applied to the output for automated detection decision and range tracking. The technique utilizes a coherent un-coded radar pulse of constant pulse duration. Two pulse repetition frequencies are used for blind speed elimination. In-phase and quadrature detection are also used. The physical implementation of the digital circuitry is modest and is judged to be within the current state-of-the-art.

A further by product of this Digital MTI is that stationary clutter is suppressed. It is to be noted that the target aircraft and the rain clutter are in the same range cell throughout this study.

Section II of this report describes the theoretical basis for Digital MTI processing and the application to aircraft detection in rain clutter. Section III details the model chosen to simulate rain characteristics. Also described in Section III is the operation of the filtering process upon sampled return signals. Section IV describes the results of the modelling with various filters. The results are presented with two conditions. The first is with no aircraft present, the second with aircraft and clutter. Section V, with references to previously published results, delineates the limitations of the Digital

6

MTI due to the rain clutter's incoherency and to quantized noise.
Conclusions are drawn in Section VI as to the problems of coherency,
and the ability of filters to reject clutter.

SECTION II

DIGITAL MTI THEORY AND DESIGN APPLICATION

2.0 SCOPE

A major problem encountered by X-Band precision approach radars
is the detection and tracking of aircraft targets in heavy rain fall.
The use of band-pass filters to separate the Doppler shifted signal
of the rapidly moving target from the clutter return of the slowly
moving rain offers a potential solution. This report presents the
results of an investigation of the ability of transversal digital
filters to improve the signal-to-rain clutter ratio. The study con-
sisted of two parts: the development of a model for the rain clutter
power density spectrum, and the implementation of a particular digital
filter. Both parts were realized on a HP-2100 Digital Computer.

The rain clutter was modelled statistically using realistic
parameters. An input clutter-to-signal ratio of 20 dB was modelled.
This clutter corresponded to a volume cell of 150 m. x 1° x 1° at
10 Km. The radar cross section of rain falling at 50 mm/hr at 10 GHz
is typically 100 m^2, for the rain cell discussed above. Typical radar
cross sections of aircraft were considered to be of the order of 1 m^2.

The digital MTI used was an n tap digital delay line characterized
by n pre-determined weights w_1, w_2,...w_n. The tap spacing corresponded
to the pulse repetition interval. The filtering operation consisted
of multiplying the complex envelope (amplitude and phase) of the com-

8

posite return signal in a given range cell from transmission 1 by w_1, from transmission 2 by w_2, etc., adding, and then computing the magnitude of the sum. The results obtained with filters of order $n = 15$, 19 and 23 are presented; the subclutter visibility improvement obtained with $n = 23$ is worthy of consideration for future system design.

This study was concerned with the extraction of targets from clutter by means of Digital Signal Processing. The basis for clutter rejection is that the centroid of the Doppler frequency distribution of the clutter power spectrum is usually well below the Doppler frequencies of aircraft targets. Thus, a moving target indicator (MTI) Digital processor is envisaged as a system that has a stop band characteristic which selectively suppresses the clutter and a pass band characteristic which embraces the target signal.

The MTI processor considered in this study could be used with a linear polarized, step scanned radar of the pencil beam type.

This investigation concentrated on the processing of the clutter and target in one representative range-azimuth-elevation cell. The system application of the technique would employ parallel processing of the other range cells, extending to 20 Km. The aggregate process would be repeated for the different azimuth elevation cells. [3] Of necessity, the signals from each range-azimuth-elevation cell must be processed in blocks of n pulses.

9

The composite radar return signals are weighted and summed. This weighting operation corresponded to processing the signals through a non-recursive digital fitler and examining the results of the weighting process after receiving n pulses. The results of the weighting process is a signal level which is to be compared with a pre-determined threshold for detection of targets for use as an MTI. This digital MTI can also be described equally as well as a transversal fitler, tapped digital delay line, n pulse canceller, etc.

2.1 Filter Characteristics

The MTI processor design had to satisfy two basic requirements for the PAR application: These were (1) a maximum range of approximately 20 Km and (2) target radial velocities between 40 and 480 knots, approximately.

A dual pulse repetition frequency (PRF) of 8.00 KHz and 5.33 KHz approximates these criteria. The maximum unambiguous range R_o as determined by the 8.00 KHz PRF is given by

$$R_o = \frac{C}{2(PRF)} = 18.75 \text{ Km.} \tag{1}$$

The blind speed, or foldover velocity, is given by

$$V_f = \lambda(PRF)/2 \tag{2}$$

which at 3.1 centimeters is 240 knots for 8.00 KHz and 160 knots for 5.33 KHz.

10

Figure 1 displays a general amplitude versus frequency character-
istic for a digital filter of the type considered. It is to be noted
that the response of a digital filter is periodic at multiples of the
PRF.

Figure 2 displays the desired amplitude versus frequency response
of filters operating at 8.00 KHz and 5.33 KHz respectively. The
purpose of the 5.33 KHz PRF and its associated filter is to fill in
the blind region (100 to 140 knots) of the 8.00 KHz filter.

2.2 Operation of Digital MTI

The MTI filtering consists first of processing n consecutive
pulses of each range bin at a PRF of 8.00 KHz using the 8.00 KHz
digital filter and then repeating the process at a rate of 5.33 KHz
using the 5.33 KHz filter. Secondly, whenever either output of the
two filters exceeds a predetermined threshold, then a target detection
decision can be invoked. The actual setting of the threshold for the
decision made upon the outputs of the filters will of course be
dictated by requirements for specific false alarm and detection
probabilities. Three cases were studied; viz, n = 15, 19, and 23.

2.3 Digital Filters

In general, the output response y at sample point n to an
arbitrary linear Digital Filter can be described by the following
equation: [4,5]

$$y(n) = - \left[a_1 \, y(n-1) + a_2 y(n-2) + a_3 \, y(n-3) + \ldots a_m \, y(n-m) \right]$$

$$+ \left[w_1 \, x(n) + w_2 \, x(n-1) + w_3 \, x(n-2) \ldots w_{r+1} \, x(n-r) \right] \qquad (3)$$

Equation 3 states that the response depends, in general, upon m past output responses and r past inputs. Non-recursive filters demand that $a_1 = a_2 = \ldots = a_m = 0$, which is the case discussed in this report.

To determine the frequency response of a sampled sinusoidal frequency as input, the Z transform is performed on Equation 3, and $e^{j\omega T}$ is substituted for Z. T is the sampling time, and ω is the angular frequency of the sinusoid.

Defining

$$X(Z) = \sum_{n=0}^{\infty} x(n) \, Z^{-n} \qquad (4)$$

$$Y(Z) = \sum_{n=0}^{\infty} y(n) \, Z^{-n} \, , \qquad (5)$$

then the system response function defined as H(Z) is

$$H(Z) = \frac{Y(Z)}{X(Z)} = \frac{\sum_{\ell=1}^{r+1} w_\ell \, Z^{-(\ell-1)}}{1} \qquad (6)$$

12

The filters used in this report had n elements or weights, thus n = r+1, in which case r=n-1 and equation 6 becomes

$$H(Z) = \sum_{\ell=1}^{n} w_\ell \ z^{-(\ell-1)} \tag{7}$$

If $e^{j\omega T}$ is substituted for Z in equation (7) then the frequency response of the filter is obtained for n samples taken at intervals of time T. Table 2 lists the actual frequency response of the various filters designed at 8.00 and 5.33 KHz., designed after the specification of Table 1.

2.4 Digital Filter Design

The filters that were designed for the MTI application under consideration were finite impulse response filters, i.e. their impulse response was non zero for a finite sample number, and exactly zero for all sample times greater than the order of the filter. Filters with finite impulse response functions exhibit Gibbs phenomena[6] in the frequency domain, i.e. the amplitude vs. frequency response have ripples due to the discontinuites in the frequency response function, or due to the finite digital impulse response function[5]. The filters used in this study were designed with the Tchebeychef[7,8,9] approximation scheme to approximate the desired pass band character-istics. Such filters have the property that, in either pass or stop bands, amplitude ripple is fixed and their phase is linear. Hence

13

the terminology, Tchebeychef equiripple, linear phase, finite impulse response filters,is used. Of the various filter designs possible, the equiripple design gives the minimum transition band between pass and stop band. [9,10,11,12] An illustration of the frequency response characteristics of such filters is shown in Figure 1. Table 1 summarizes the properties of the various filters that were designed and tested in this report. Table 2 tabulates the actual filters' performance as a function of radial velocity. Table 3 lists the filter weights used in this report whose frequency response is tabulated in Table 2.

SECTION III

RAINFALL CLUTTER MODELLING AND MTI OUTPUT

3.0 MONTE CARLO SIMULATION OF CLUTTER AND TARGET

The performance of the various order filters was evaluated by simulating the amplitude, phase, and velocity of both rain drops and targets by means of a Monte Carlo. A simple multiplication of the filter power spectrum by the power spectrum of rain clutter return signal is not appropriate in unraveling the clutter's rejection in the presence of signal, because the power spectrum of clutter is statistical in nature.

The complex radar return from an assembly of M scatterers and a target at time t is given by Equation 8.

$$R(t) = \sum_{k=1}^{M} (A_k \, e^{j\phi_k} \, e^{j\frac{4\pi V_k t}{\lambda}}) + \sqrt{\sigma_T} \; e^{j\frac{4\pi V_T t}{\lambda}} \, e^{j\phi_T} \qquad (8)$$

M = number of rain drops in fiducial volume

ϕ_k is the initial phase at $t = 0$ of the kth drop ($\phi_k = \frac{4\pi R_k}{\lambda}$, R_k radial distance to k^{th} drop)

V_k is the velocity of the kth drop.

A_k is the amplitude of power return of kth drop, such that

15

$$\left< \left| \sum_{k=1}^{M} |A_k|^2 \right| \right> = 20 \text{ dB} \tag{9}$$

σ_T is the target cross section and is such that $\langle \sigma_T \rangle = 0$ dB,

ϕ_T is the initial phase of the target $(4\pi R_T/\lambda)$, where

R_T is the radial distance of the target.

Both the target's initial phase and the initial phase of the scatterers are assumed to be statistically independent and uniformly distributed, viz,

$$p(\phi) \ d\phi = \frac{d\phi}{2\pi} \ . \tag{10}$$

In the Rayleigh limit $(D \ll \lambda)$ [13,14] the amplitude A_k must vary as the cube of the diameter. The diameter follows a Marshall-Palmer distribution [15,16],

$$N(D)dD = e^{-\Lambda D} \ d(D\Lambda) \tag{11a}$$

$$\Lambda = 4.1 \ R^{-.21}, \tag{11b}$$

where Λ is in units of mm^{-1} and R, the rain rate, is in units of mm/hr.

16

3.1 Rain Clutter Cross Section Model

The (total differential) cross section of rain drops, approximated by dielectric spheres,is in the Rayleigh limit (diameter/wavelength << 1), given [1.3] by

$$\sigma(\theta) = (\frac{2\pi a}{\lambda})\ 4\pi a^2\ \frac{n^2 - 1}{n^2 + 2}\ \frac{3}{8}\ (1 + \cos^2 \theta) \cdot \sin \theta \qquad (12)$$

where:

a = radius of sphere

λ = wavelength of incident radiation

n = complex index of refraction of dielectric

$$n^2 = \varepsilon + j\ \frac{4\pi\delta}{\omega} \qquad (13)$$

ε = dielectric constant $\sim \sqrt{1.333}$

δ = conductivity ~ 0

$\omega = 2\pi f = 2\pi\ \frac{c}{\lambda}$ = angular frequency of radiation.

$$\sigma_{tot} = \int_{o}^{\pi} \sigma(\theta)\ d\theta\ = (\frac{2\pi a}{\lambda})^4\ 4\pi a^2 \left|\frac{n^2 - 1}{n^2 + 2}\right|^2 \qquad (14)$$

Defining

$$|K|^2 = \left|\frac{n^2 - 1}{n^2 + 2}\right|^2\ , \qquad (15)$$

17

it is found that $|K|^2 = .9275$ at 20°C at a wavelength of 3.21 cm, whereas at 0°C, $|K|^2 = .9300$ [14].

An average diameter for heavy rain [15, 16] (50 mm per hour) is .1 cm(2) which yields an average total back scatter cross section of 3.45×10^{-10} m^2. In a fiducial volume of 5×10^6 m^3 there are 3×10^{11} rain drops, which translates to a cross section of 100 m^2. (Fiducial volume $1^{\circ} \times 1^{\circ} \times 1$ us at 10 KM). Small aircraft cross sections considered in this report are in the neighborhood of 1 m^2. Thus a clutter to signal ratio for the rain and the aircraft considered is of the order of 20 dB.

3.2 Rain Velocity Distribution Model

The velocity spectrum of rain drops has been hypothesized [17] to be a Gaussianly distributed spectrum. The width of the distribution is ascribed to four effects

$$\sigma_v^2 = \sigma_{Shear}^2 + \sigma_{Beam}^2 + \sigma_{Turb.}^2 + \sigma_{Fall}^2, \tag{16}$$

and in general

$$|\sigma_{Shear}| < |\sigma_{Beam}| > |\sigma_{Turb.}| > |\sigma_{Fall}| \tag{17}$$

Appendix A presents an analysis of the origin as an order of magnitude calculation of the various terms. Suffice it to say that, $\sigma_v < 2 \frac{m}{sec}$ in thunderstorms. The important feature of σ_{Shear} is that it is linearly proportional to the range of observation and is, for near horizontal scanning, the dominant contribution to the variance of the Doppler spectrum.

18

3.3 Filter Operation

Three filters of order n = 15, 19, and 23 respectively were used as weights in a Digitized MTI filter. Since in the system design application two PRF's are to be employed as noted in Section 2.1, there were three filters implemented at each of the PRFs

Denoting the response of filter i, $1 \leq i < 6$ as F_i, the response of filter i to samples of the composite radar return signal (I, and Q, or Amplitude and Phase) given in Equation (8) is

$$F_i = \left| \sum_{\ell=1}^{n} R(\ell)\, w_i(\ell) \right| \qquad (18)$$

The index ℓ, in referring to $R(\ell)$, denotes the sample of the composite signal at time ℓT_s where T_s is the sampling time, which is also the PRI (pulse repetition interval).

Thus,

$$R(\ell) = \sqrt{\sigma_T}\; e^{j\phi_T}\, e^{j\,\frac{4\pi V_T T_s \ell}{\lambda}} +$$

$$\sum_{m=1}^{M} A_m\, e^{j\phi_m}\, e^{j\,\frac{4\pi V_m T_s \ell}{\lambda}} \qquad (19)$$

Denoting W(k), $1 \leq k \leq n$, as the equi-spaced sample response of the digital filter in the frequency domain, then the finite impulse response function, $w(\ell)$, used as weights in the transversal

filters considered in this report, is obtained by the Discrete Fourier Transform

$$w(\ell) = \frac{1}{n} \sum_{k=1}^{n} W(k) \ e^{-j \frac{2\pi \ell k}{n}} \tag{20}$$

The inverse transform of the impulse response function is

$$W(k) = \sum_{\ell=1}^{n} w(\ell) \ e^{j \frac{2\pi \ell k}{n}} \tag{21}$$

3.4 Interpretation of Filter Response

In the special case of no clutter, $A_k = 0$, in Equation 8 and for a target cross section $\sigma_T = 1$, the response of the filter F_i is

$$F_i = \left| \sum_{\ell=1}^{n} R(\ell) \ w_i(\ell) \right| \tag{22a}$$

$$= \left| \sum_{\ell=1}^{n} e^{j\phi_T} \ e^{j \frac{4\pi V_T T_s \ell}{\lambda}} \ w_i(\ell) \right| \tag{22b}$$

$$= \left| \sum_{=1}^{n} w_i(\ell) \ e^{j \frac{4 V_T T_s \ell}{\lambda}} \right| . \tag{22c}$$

Moreover, this is the amplitude of the Digital Filter's response at a Doppler frequency $2v/\lambda$, as Equation 22c is just the Discrete Fourier Transform of the filter's weights.

20

SECTION IV

DESCRIPTION OF RESULTS

4.0 RESULTS

Program Implementation

The filters were tested with two sets of boundary conditions.
The first involved generating clutter whose Doppler characteristics
were Gaussian with a mean radial velocity of $10 \frac{m}{Sec}$ (20 knots) and
whose spectral width (standard deviation) was 1 m/sec. The clutter
had an average power of 20 dB. The second condition had the same
clutter characteristics, but in addition had a target with a power
return of 0 dB and a radial velocity of 50 m/sec (100 knots), cf.
Equation (8).

Figures 3 and 4 illustrate the statistics of the real (I channel)
and the imaginary (Q-Channel) parts of the sampled received signal.

The power p returned (sum of squares of I and Q) had statistics
that are exponentially distributed

$$\frac{df}{dp} = \bar{e} \; p/<p> \; \frac{dp}{<p>} \tag{23}$$

where <p> was 20 dB.

If, as in the second case, there was a target present, then the
average return clutter to signal power was 20 dB. In taking the square
root of the power spectrum, the Rayleigh spectrum of amplitude is
observed.

21

$$\frac{df}{dA} = 2A \; \bar{e} \; {}^{A^2/<A^2>} \; \frac{dA}{<A^2>} \; , \; A = \sqrt{p} \; . \tag{24}$$

Figures 3 through 6 are samples of I, Q, power and amplitude drawn from 500 independent ensembles of rain scatterers and targets described by Equation (8). Both the power spectrum and the amplitude spectrum are displayed in Figures 5 and 6.

Figures 7 to 12 are 8 KHz filters with 15, 19, and 23 elements . Figures 13 to 18 are 5.33 KHz filters with 15, 19, and 23 elements respectively. Figures 7 through 18 alternate the boundary condition of clutter only with clutter plus target.

These figures are histograms with the vertical scale relating the number of occurrences and the horizontal scale, the amplitude output of the filter. Note, if clutter were absent and the signal were in the passband, then (since $\sigma_T = 1$) the output of the filter is $1 \pm \delta p$ (cf Figure 1 and Table 1), the particular value depending solely upon the given Doppler frequency.

Conclusions can be drawn from these figures regarding the probability of detection when an aircraft is present by selecting a threshold level. However, when the threshold is chosen and no target is present, false alarm probabilities can only be grossly estimated due to the limited statistics. The information to be learned from the figures is in their internal comparisons, i.e., increasing the filter elements sharpens the response (more processing time means better frequency selectivity).

22

SECTION V

PROCESSING LIMITATIONS

5.0 SIGNAL CORRELATION

Nathinson and Reilly[17] have obtained data in severe rain storms ($\approx$ 40 mm/hr) that tend to support the notion of Gaussianly distributed spectra. Appendix B derives an auto correlation function, with the assumption that individual scatterers have velocity distributed Gaussianly.

In the continuous case the lagged products are defined as

$$\rho_{II}(\tau) = \frac{\int I(\tau)\ I(t+\tau)\ dt}{\int I(\tau)\ I(\tau)\ dt} \tag{25}$$

$$\rho_{IQ}(\tau) = \frac{\int I(t)\ Q(t+\tau)\ dt}{\int I(t)\ I(t)\ dt}, \tag{26}$$

where $\qquad I(t) = R_e(R(t)),$ (27a)

and $\qquad Q(t) = I_m(R(t))$ (27b)

In the Discrete (sampled) case, the lagged products are defined (with k and L multiples of the PRI) as:

$$\rho_{II}(\tau) = \frac{\sum_{k=1}^{N} I(k)\ I(k+L)}{\sum_{k=1}^{N} I(k)\ I(k)}$$

23

$$\rho_{IQ}(\tau) = \frac{\sum\limits_{k=1}^{N} I(k) \; Q(k+L)}{\sum\limits_{k=1}^{N} I(k) \; I(k)} \tag{29}$$

The function $\rho(\tau)$ is also defined as

$$\rho(\tau) = \sqrt{\rho_{II}^2(\tau) + \rho_{IQ}^2(\tau)} \tag{30}$$

It is proved in the appendix that for Gaussianly distributed velocities that:

$$\rho(\tau) = e^{-\frac{1}{2} \left(\frac{4\pi\tau\sigma_v}{\lambda}\right)^2} , \tag{31}$$

$$\rho_{II}(\tau) = \cos\left[\frac{4\pi <v> \tau}{\lambda}\right] \cdot \rho(\tau) , \tag{32}$$

$$\rho_{IQ}(\tau) = \sin\left[\frac{4\pi <v> \tau}{\lambda}\right] \cdot \rho(\tau) \tag{33}$$

24

Thus, $\rho(\tau)$ is the correlation function of the fluctuations, with the average Doppler term removed. The Fourier transform of $\rho(\tau)$ displays the fluctuation spectrum:

$$S(f) = \left| \int e^{-j2\pi f\tau} \rho(\tau) d\tau \right|^2 \tag{34a}$$

$$S(f) = \frac{\lambda/2}{\sqrt{2\pi} \; \sigma_v} \tag{34b}$$

Thus, the breadth of the distribution is governed by $2\sigma_v/\lambda$, viz, its width varies linearly with the variance of the Doppler spectrum and inversely proportional to the wavelength. Typical values of σ_v are 1 to 2 m/sec, and with $\lambda = 3$ cm, the width of the fluctuation spectrum is 66 or 133 Hz for σ_v of 1 or 2 $\frac{m}{sec}$ respectively.

Either equation 32 or 33 will allow a determination of the average Doppler velocity shift due to the cosine or sine term of $\frac{4\pi \bar{V} \tau}{\lambda}$.

Figures 19 and 20 display both $\rho_{II}(\tau)$ and $\rho(\tau)$, which was obtained from the data of J. Roberts[19]. Reberts had digitized signals of Nathanson's experiment on collecting I and Q signals of rain storms. The radar had a wavelength $\lambda = 5.2$ cm, and a PRF = 1.25 KHz. Thus, from $\rho_{II}(\tau)$, the average velocity is approximately $\langle V \rangle \sim 3.25$ m/sec = 6.5 knots, and the width $\sigma_v = \langle (V - \langle V \rangle)^2 \rangle^{\frac{1}{2}}$ is approximately 1 m/sec.

With a knowledge of the correlation time determined by $\rho(\tau)$, an upper limit is placed upon coherent processing of signals determined

25

by the widths of Doppler velocity spectra. Or stated in the frequency domain, the width of the Doppler spectra is governed solely by the width of the velocity spectra, and this width placed the upper limit upon a filter's rejection capabilities, i.e. the amount of power that is within the pass band is determined not only by the central Doppler frequency, but also by the width of the Doppler spectrum (as is expected).

Using Equation 31, an estimate of the upper limit of the processing time can be made as follows. If the correlation of the signal from the beginning to the end of the processing is .1, then for a wavelength of 3 cm, and $\sigma_v = \frac{1m}{sec}$ $\tau = \frac{\lambda}{4\pi\sigma_v}$ $\sqrt{-2\ln .1} = 5.2$ m sec. This corresponds to a 41 element filter at 8 KHz and 27 elements at 5.33 KHz.

5.1 Quantized Noise

The process of sampling and digitizing an analog signal introduces noise (random error) into the signal that is being analyzed. The noise is due to the quantization of the analog signal.

Appendix C discusses the necessary conditions for the noise to be considered white noise, viz, that successive signals being digitized are uncorrelated within a quantum level. A derivation of the ratio of white noise due to quantization of the true signal is presented in the appendix. The ratio of quantized noise power to received power for a 10 bit converter is -52 dB, an 11 bit converter is -58 dB, etc.

26

SECTION VI

CONCLUSIONS

Digital filters with increasing elements, but having approximately the same frequency response characteristics, perform better on suppressing clutter than filters with a smaller number of elements. It is also of importance to note that the processing time should not be greater than the time determined by the autocorrelation of the clutter to be suppressed. If the processing time exceeds the coherence time of clutter, then the digital filter will be processing parts of the data stream that are statistically independent of the preceding portion; hence the filter will be used as an incoherent device. Stated in context of an X-Band radar, the signal processing must be done in a time of the order of 5.0 milliseconds if the spectral width of the clutter is 1 m/sec.

TABLE 1

FILTER DESIGN CHARACTERISTICS

All Entries Refer to Figure 1

N	f_1	f_2	f_2-f_1	δ_p	δ_s	f_1	f_2	f_2-f_1	δ_p	δ_s
15	.398	1.333	.935	1.03	-48.02	.670	1.333	.664	1.04	-47.94
19	.626	1.333	.707	1.03	-48.00	.821	1.333	.502	1.04	-47.93
23	.7674	1.333	.576	1.04	-47.98	.932	1.333	.401	1.05	-47.89

 8.0 KHz Filters   5.33 KHz Filters

frequency in Kilohertz

δ_p, δ_s in dB

N is the order of the filter

Note $V = \lambda f/2$,   thus 1.333 KHz

corresponds to a Doppler velocity of 20 $\frac{m}{sec}$ @ λ = 3 cm.

28

TABLE 2

Frequency Reponse of Filters (dB) versus Radial Velocity for λ = 3 cm

V_R ORDER	8.00 KHz			5.33 KHz		
	15	19	23	15	19	23
0 m/sec	−48.	−48.	−48.	−48	−48.	−54.
10	−17.7	−37.1	−48.	−50.5	−60	−59
20	−.5	−.5	−.6	−.6	−.6	−.6
30	−.4	−.5	+.02	−.03	+.5	+25
40	+.46	+.02	−.3	−.5	+.5	−.56
50	−.5	+.4	−.5	−.3	+.46	+.25
60	+.5	−.5	+.02	−.6	−.6	−.6
70	−.5	+.4	−.4	−50.5	−60.	−59
80	+.5	+.02	−.2	−48.	−48.	−48
90	−.3	−.5	+.02	−50.5	−60.	−54
100	−.5	−.5	−.5	−.6	−.6	−.6
110	−17.7	−37.1	−48	−.03	+.5	+.25
120	−48.	−48.	−48	−.56	+.5	−.56
130	−17.7	−37.1	−48	−.3	+.46	+.25
140	−.5	−.5	−.6	−.6	−.6	−.6
150	−.4	−.5	+.02	−50.5	−60.	−54.
160	+.46	+.02	−.3	−48.	−48.	−48.
170	−.5	+0.4	−.5	−.6	−.6	−.6
180	.5	−.5	−.5	−.6	−.6	−.6
190	−.5	+.4	−.4	−.3	+.4	+.3
200	+.5	+.02	−.2	−.6	+.5	−.6
210	−.4	−.5	+.02	−.3	+.46	+.25
220	−.5	−.5	−.5	−.6	−.6	−.6
230	−17.7	−37.1	−48.	−50.5	−60.	−54.
240	−48.	−48.	−48.	−48.	−48.	−48.

$$V_R = \frac{\lambda f_D}{2}$$

λ = 3 cm., f_D is Doppler frequency from target with Radial Velocity V_R in m/sec.

TABLE 3

FILTER WEIGHTS

	8.00 KHz n=15	5.33 KHz n=15
W(1)	−·005067	.010351
W(2)	+.041367	−.035465
W(3)	+.025585	−.0044975
W(4)	−.00634	+.05458
W(5)	−.069283	+.05698
W(6)	−.14857	−.082521
W(7)	−.21513	−.2988
W(8)	+.75885	.59474

Where terms greater than 8 have been omitted and are related by $W(16-k) = W(k)$, $1 \leq k \leq 8$.

TABLE 3 (Cont'd)

	8.00 KHz n=19	5.33 KHz n=19
W(1)	-.0097096	-.011098
W(2)	-.027526	.029622
W(3)	.021661	.000133
W(4)	.033945	-.035468
W(5)	.043443	-.021503
W(6)	.012459	.0524
W(7)	-.05868	.075366
W(8)	-.15262	-.066455
W(9)	-.23279	-.30694
W(10)	+.73566	.57191

$$W(20-k) = W(k), \quad 1 \leq k \leq 10$$

31

TABLE 3 (Cont'd)

	8.00 KHz	5.33 KHz
	n=23	n=23
W(1)	.023511	.011699
W(2)	-.016915	-.026468
W(3)	-.022938	.0013783
W(4)	-.017912	.025923
W(5)	.0049624	.010138
W(6)	.036139	-.036618
W(7)	.051167	-.033569
W(8)	.024877	.047031
W(9)	-.050044	.085507
W(10)	-.15301	-.054856
W(11)	-.24261	-.31104
W(12)	.7219	+.55771

$$W(24-k) = W(k), \ 1 \leq k \leq 12$$

33
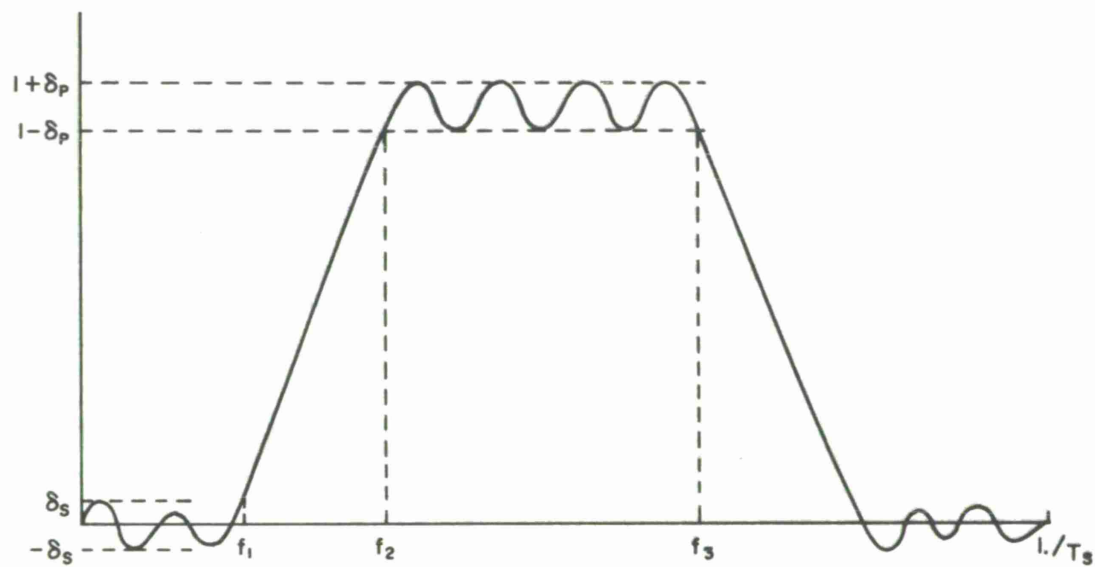
$f_2 - f_1$ = TRANSITION WIDTH

T_S = SAMPLING TIME

$1./T_S$ = SAMPLING FREQUENCY

δ_S = MAXIMUM DEVIATION IN STOP BAND

δ_P = MAXIMUM DEVIATION IN PASS BAND

f_3 = $T_S^{-1} - f_2$

Figure I CHARACTERISTIC OF EQUIRIPPLE DIGITAL FILTER
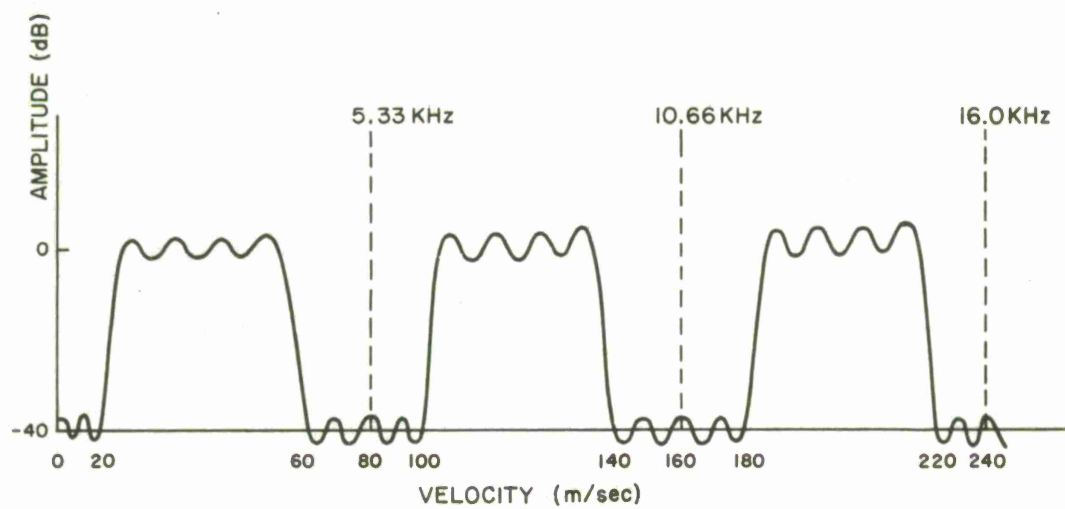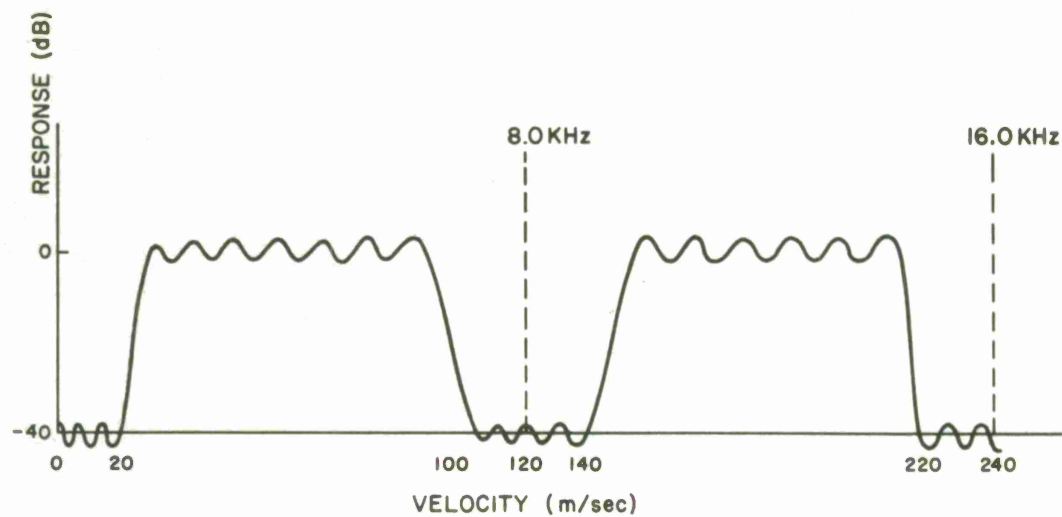
Figure 2 AMPLITUDE RESPONSES OF 8.00 KHz AND 5.33 KHz FILTERS

IA-43,258

34

```
         XX++++++++XX+++++++++XX+++++++++XX++++++++++XX+++++++++XX
    50   X                                                              X
         +                                                              +
         +                                                              +
         +                    2 1                                       +
         +                    X X  2   2                                +
         +                    X X31X1X3X3                               +
         +                  43X2XXXXXXXXXX4X X                          +
         +           2    3XXXXXXXXXXXXXXXX3X41 1                        +
         +           2 X3 XXXXXXXXXXXXXXXXXXXXXXX                        +
         X        13 34X3XXXXXXXXXXXXXXXXXXXXXXXXXXX331 22               X
     0   XX++++++++XX+++++++++XX+++++++++XX++++++++++XX+++++++++XX
       -.250E+02 -.150E+02 -.500E+01  .500E+01  .150E+02
```

UNDERFLOW =   0 TOTAL =   500 OVERFLOW =   0
    AVERAGE =   .292 STANDARD DEVIATION =   7.239

Each X Represents 5

FIGURE 3   STATISTICS OF I CHANNEL

```
       XX++++++++XX++++++++XX++++++++XX++++++++XX++++++++XX
   50  X                                                  X
       +                                                  +
       +                                                  +
       +                     X                            +
       +                  3  2X3                          +
       +                 4X33XXX4 4 1                      +
       +               4 XXXXXXXXXX4X                      +
       +             3  3 4XXXXXXXXXXXXXXXX4441            +
       +             X44X3XXXXXXXXXXXXXXXXXXXX112          +
       X       31  33XXXXXXXXXXXXXXXXXXXXXXXXXXX4243X211   X   -
    0  XX++++++++XX++++++++XX++++++++XX++++++++XX++++++++XX
       -.250E+02 -.150E+02 -.500E+01  .500E+01  .150E+02
```

UNDERFLOW =   0 TOTAL =   500 OVERFLOW =   0
   AVERAGE =   -.402 STANDARD DEVIATION =   7.450

Each X Represents 5

FIGURE 4   STATISTICS OF Q CHANNEL

```
        XX++++++++XX+++++++++XX+++++++++XX++++++++XX++++++++XX
   50   X                                                        X
        +2                                                       +
        +X4                                                      +
        +XX 3                                                    +
        +XXXX 2311                                               +
        +XXXXXXXXX                                               +
        +XXXXXXXXX4X   1                                         +
        +XXXXXXXXXXXX2X1111  2                                   +
        +XXXXXXXXXXXXXXXXXXX       1                             +
        XXXXXXXXXXXXXXXXXXXXXXXXX3X44X42X214    3313 12 1   1 X
    0   XX++++++++XX+++++++++XX+++++++++XX++++++++XX++++++++XX
     .000E+00 1.000E+02  .200E+03  .300E+03  .400E+03
```

UNDERFLOW =   0 TOTAL =   499 OVERFLOW =   1
    AVERAGE =   106.984 STANDARD DEVIATION =   95.308

Each X Represents 5

FIGURE 5   STATISTICS OF RECEIVED POWER

```
          XX++++++++XX++++++++XX++++++++XX++++++++XX++++++++XX
   100    X                                                  X
          +                                                  +
          +                                                  +
          +                                                  +
          +                                                  +
          +                                                  +
          +                                                  +
          +                                                  +
          X            2                                     X
    50    X            X                                     X
          +            X1                                    +
          +        4 1 XX1                                   +
          +        X XXXXX3                                  +
          +        XXXXXXXX X                                +
          +       XXXXXXXXXXX4                               +
          + 21XXXXXXXXXXXXXX                                 +
          + XXXXXXXXXXXXXX34                                 +
          + XXXXXXXXXXXXXXXX 21                              +
          X4XXXXXXXXXXXXXXXXXX4XX11 1                        X
     0    XX++++++++XX++++++++XX++++++++XX++++++++XX++++++++XX
        ,000E+00 1,000E+01  ,200E+02  ,300E+02  ,400E+02
```

UNDERFLOW =   0 TOTAL =   500 OVERFLOW =   0
   AVERAGE =   9.312 STANDARD DEVIATION =   4.605
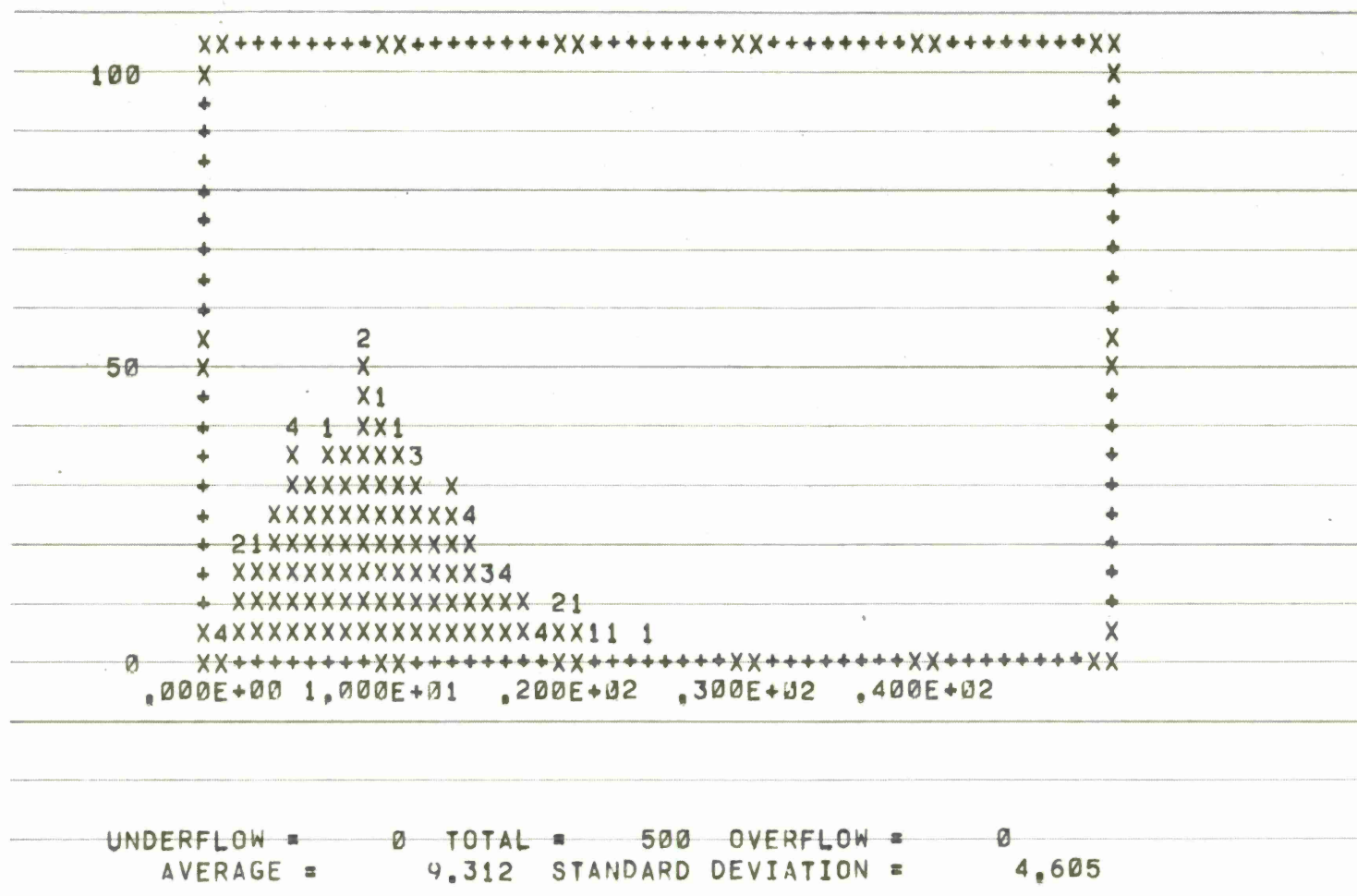
Each X Represents 5

FIGURE 6   STATISTICS OF RECEIVED AMPLITUDE

```
       XX++++++++XX++++++++XX++++++++XX++++++++XX++++++++XX
  50   X                                                  X
       +                                                  +
       +                                                  +
       +                                                  +
       +                                                  +
       +                                                  +
       +                                            X     +
       +         1      2 3X122      1 X41    X3 1  1      +
       +      4 3 X1342X4XXXXXX44XXXXXXXX4X4XX3X3 X23442+
       X   222X334X4XXXXXXXXXXXXXXXXXXXXXXXXXXXXX4XXXXXXX
   0   XX++++++++XX++++++++XX++++++++XX++++++++XX++++++++XX
      .000E+00  .400E+00  .800E+00  .120E+01  .160E+01
```

```
UNDERFLOW =      0  TOTAL =    424  OVERFLOW =     76
    AVERAGE =        1.146  STANDARD DEVIATION =        .476
```
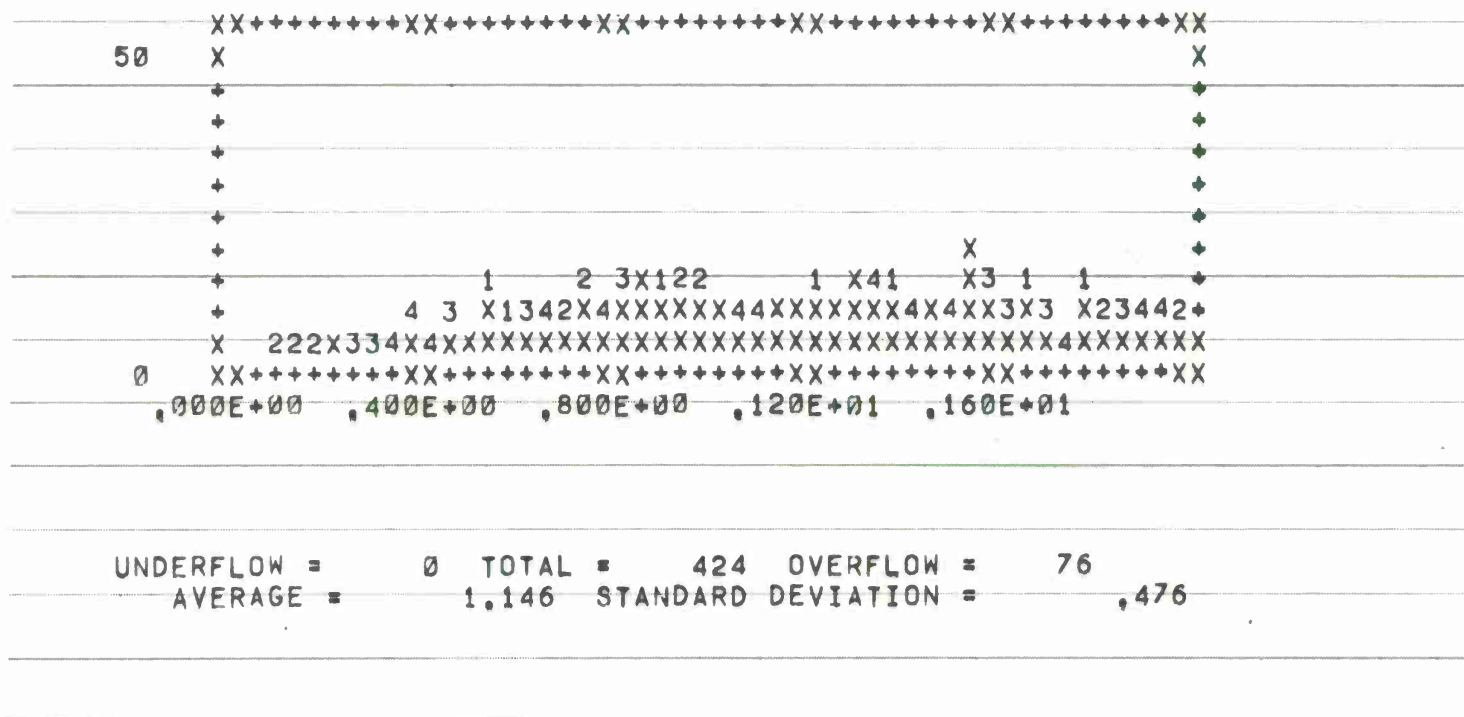
Each X Represents 5

FIGURE 7   OUTPUT STATISTICS OF 15 ELEMENT FILTER WITH PRF OF 8Khz, CLUTTER ONLY

```
           XX+++++++XX+++++++XX+++++++XX+++++++XX+++++++XX+++++++XX
  50       X                                                      X
           +                                                      +
           +                                                      +
           +                                                      +
           +                                                      +
           +                   1                 3                +
           +                   X  2       1   X   X        2    1 +
           +           2 2233 1X34X44X2  X1  4X34X42 211X4424X113+
           X    2 413XXXX4XXXX2XXXXXXXXXXXX4XXXXXXXXXXXXXXXXXXXXXX
   0       XX+++++++XX+++++++XX+++++++XX+++++++XX+++++++XX+++++++XX
         .000E+00   .400E+00   .800E+00   .120E+01   .160E+01


    UNDERFLOW =      0  TOTAL =     356  OVERFLOW =     144
       AVERAGE =        1,149  STANDARD DEVIATION =        ,489
```

Each X Represents 5

FIGURE 8   OUTPUT STATISTICS OF 15 ELEMENT FILTER WITH PRF OF 8Khz, TARGET PLUS CLUTTER

40

Each X Represents 5

FIGURE 9   OUTPUT STATISTICS OF 19 ELEMENT FILTER WITH PRF OF 8.0 Khz, CLUTTER ONLY

```
      XX+++++++++XX++++++++++XX+++++++++XX+++++++++XX+++++++++XX
  50  X                                                       X
      +                        3   2                          +
      +                        X   X    3                     +
      +                        X2XX     X                     +
      +                        XXXX3XXX4                      +
      +                 3   XXXXXXXXX2                        +
      +                 X14XXXXXXXXXX                         +
      +              1XXXXXXXXXXXXX233 X                       +
      +              XXXXXXXXXXXXXXXXXX XX                     +
      X         22  2123XXXXXXXXXXXXXXXXXXX3XX342 31 1         X
   0  XX+++++++++XX++++++++++XX+++++++++XX+++++++++XX+++++++++XX
      .000E+00   .400E+00   .800E+00   .120E+01   .160E+01
```

UNDERFLOW =   0   TOTAL =   500   OVERFLOW =   0
     AVERAGE =   .989   STANDARD DEVIATION =   .228

Each X Represents 5

FIGURE 10   OUTPUT STATISTICS OF 19 ELEMENT FILTER WITH PRF OF 8.0Khz, TARGET PLUS CLUTTER

```
     XX++++++++++XX++++++++++XX++++++++++XX++++++++++XX++++++++++XX
300  X                                                            X
     +                                                            +
     +                                                            +
     +                                                            +
     +                                                            +
     +9                                                           +
     +X                                                           +
     +X                                                           +
     XX                                                           X
200  XX                                                           X
     +X                                                           +
     +X5                                                          +
     +XX                                                          +
     +XX                                                          +
     +XX                                                          +
     +XX                                                          +
     +XX                                                          +
     +XX                                                          +
     XXX                                                          X
100  XXX                                                          X
     +XX                                                          +
     +XX                                                          +
     +XX                                                          +
     +XX7                                                         +
     +XXX                                                         +
     +XXX                                                         +
     +XXX                                                         +
     +XXX7                                                        +
     XXXXX63111                                                   X
  0  XX++++++++++XX++++++++++XX++++++++++XX++++++++++XX++++++++++XX
     .000E+00   .400E+00   .800E+00   .120E+01   .160E+01
```

UNDERFLOW =   0   TOTAL =   500   OVERFLOW =   0
    AVERAGE =   .052   STANDARD DEVIATION =   .042

Each X Represents 10
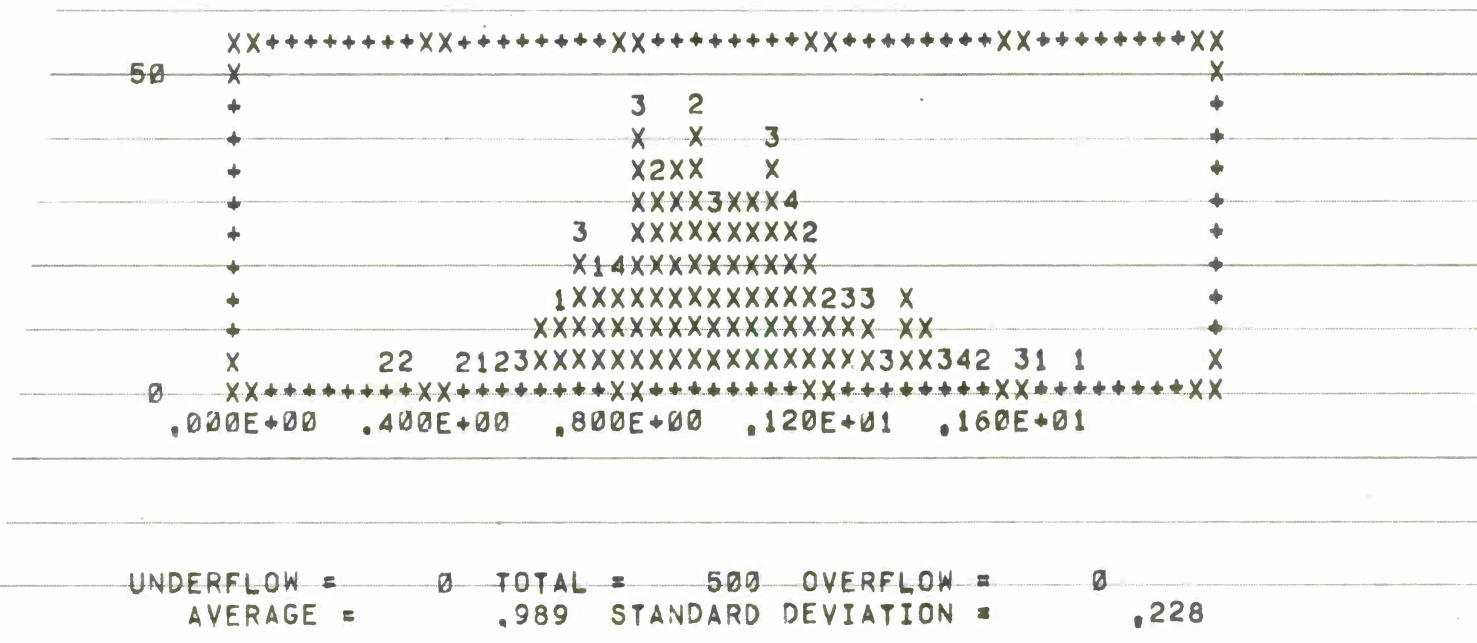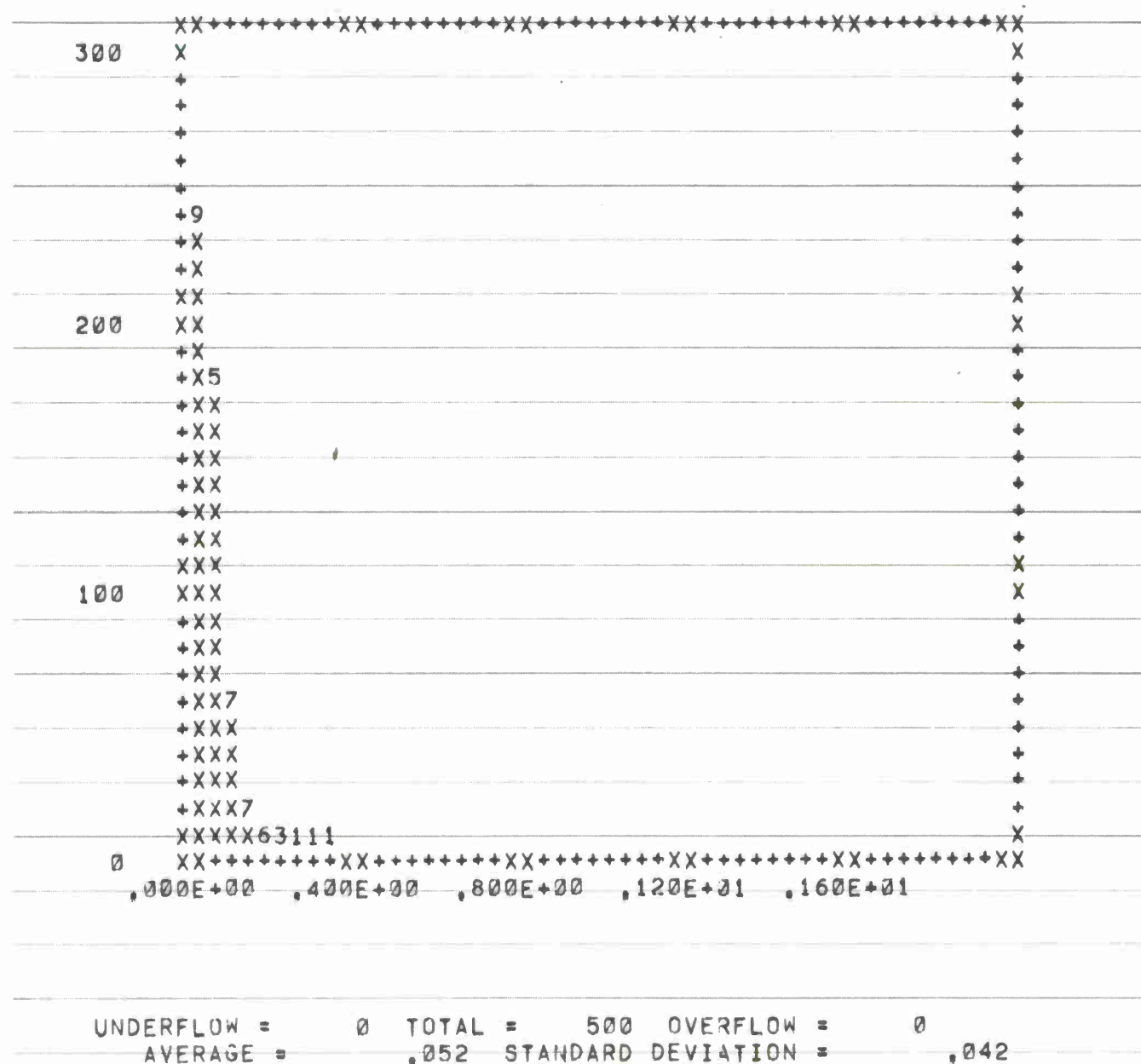
FIGURE 11   OUTPUT STATISTICS OF 23 ELEMENT FILTER WITH PRF OF 8.0Khz, CLUTTER ONLY

```
300   X                           X                           X
      +                           +                           +
      +                           +                           +
      +                           +                           +
      +                           +                           +
      +                           +                           +
      +                1          +
      +                X          +
      X                X          X
200   X                X          X
      +                X          +
      +                X          +
      +                X          +
      +                X          +
      +                X          +
      +                X          +
      +                X          +
      +                X          +
      X              3X4          X
100   X              XXX          X
      +              XXX          +
      +              XXX          +
      +              XXX          +
      +              XXX          +
      +              XXX          +
      +              XXX          +
      +            2XXX6          +
      +            XXXXX          +
      X        26XXXXXX321        X
  0   XX++++++++XX++++++++XX++++++++XX++++++++XX++++++++XX
     .000E+00  .400E+00  .800E+00  .120E+01  .160E+01
```

UNDERFLOW =   0   TOTAL =   500   OVERFLOW =   0

AVERAGE =   .943   STANDARD DEVIATION =   .048

Each X Represents 10

FIGURE 12   OUTPUT STATISTICS OF 23 ELEMENT FILTER WITH PRF OF 8.0Khz, TARGET PLUS CLUTTER

```
        XX++++++++XX+++++++++XX+++++++++XX+++++++++XX+++++++++XX
  100   X                                                      X
        +                                                      +
        +      4                                               +
        +      X                                               +
        +     4X                                               +
        +     XX                                               +
        +   3XX34                                              +
        +   XXXXX                                              +
        +   XXXXX                                              +
        X   XXXXX                                              X
   50   X   XXXXX                                              X
        +   XXXXX                                              +
        +   XXXXX3                                             +
        +   XXXXXX                                             +
        +   XXXXXX                                             +
        +3XXXXXX21                                             +
        +XXXXXXXXX                                             +
        +XXXXXXXXX1                                            +
        +XXXXXXXXXX2                                           +
        XXXXXXXXXXXX2 2   1                                    X
    0   XX++++++++XX+++++++++XX+++++++++XX+++++++++XX+++++++++XX
     .000E+00   .400E+00   .800E+00   .120E+01   .160E+01
```
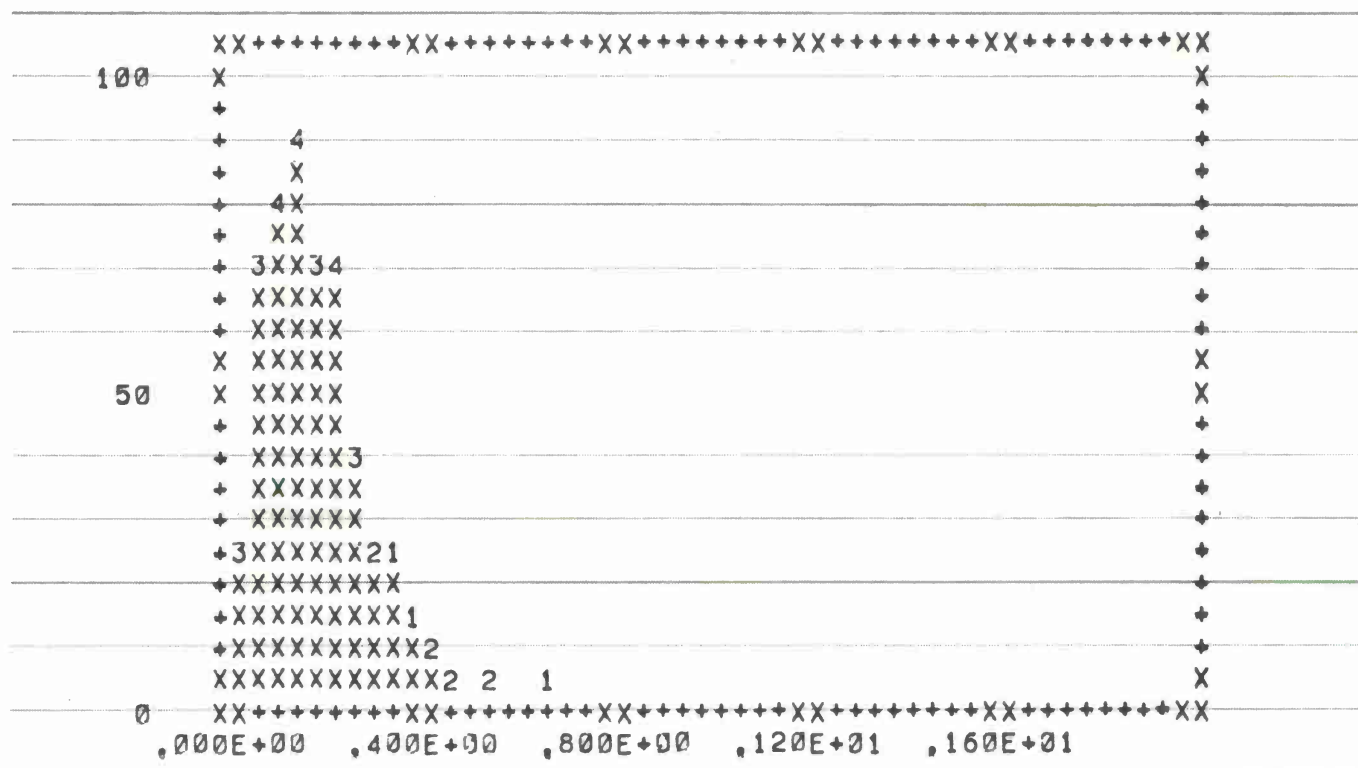
```
   UNDERFLOW =      0  TOTAL =    500  OVERFLOW =      0
        AVERAGE =        .171  STANDARD DEVIATION =        .099
```

Each X Represents 5

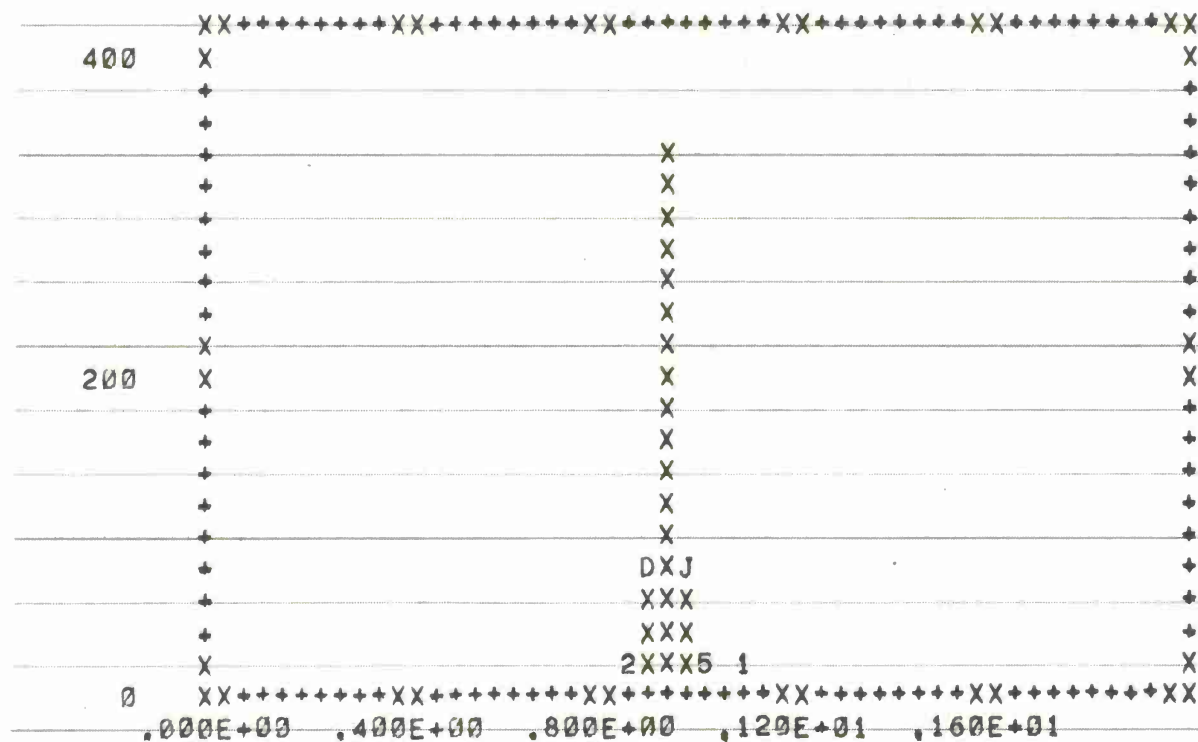FIGURE 13   OUTPUT STATISTICS OF 15 ELEMENT FILTER WITH PRF OF 5.33 Khz, CLUTTER ONLY

```
       XX++++++++XX++++++++XX++++++++XX++++++++XX++++++++XX
100    X                                                  X
       +                                                  +
       +                                                  +
       +                                                  +
       +                                                  +
       +                3                                 +
       +                X                                 +
       +                X                                 +
       +              4 X                                 +
       X              X.4X                                X
50     X              XXX3                                X
       +              XXXXX                                +
       +              XXXXX4                               +
       +            2XXXXXX1                               +
       +            XXXXXXX                                +
       +          3XXXXXXXX4                               +
       +          2XXXXXXXXXX                              +
       +          XXXXXXXXXXX                              +
       +        43XXXXXXXXXXXX                             +
       X    !13XXXXXXXXXXXXXXX422121 1                     X
0      XX++++++++XX++++++++XX++++++++XX++++++++XX++++++++XX
     .000E+00   .400E+00   .800E+00   .120E+01   .160E+01
```

UNDERFLOW =   0 TOTAL =   500 OVERFLOW =   0
   AVERAGE =   .950 STANDARD DEVIATION =   .141
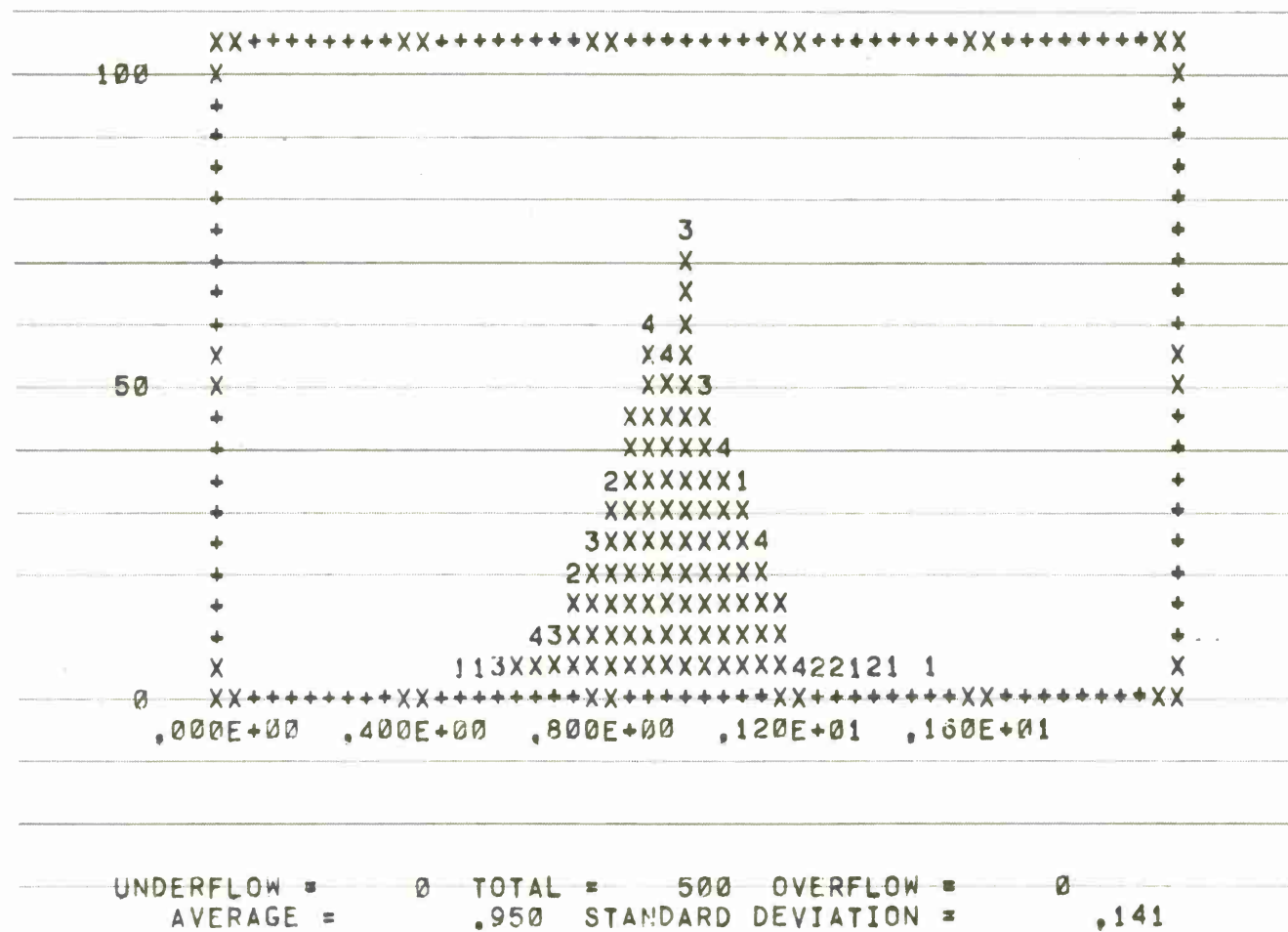
Each X Represents 5

FIGURE 14   OUTPUT STATISTICS OF 15 ELEMENT FILTER WITH PRF OF 5.33 Khz, TARGET PLUS CLUTTER
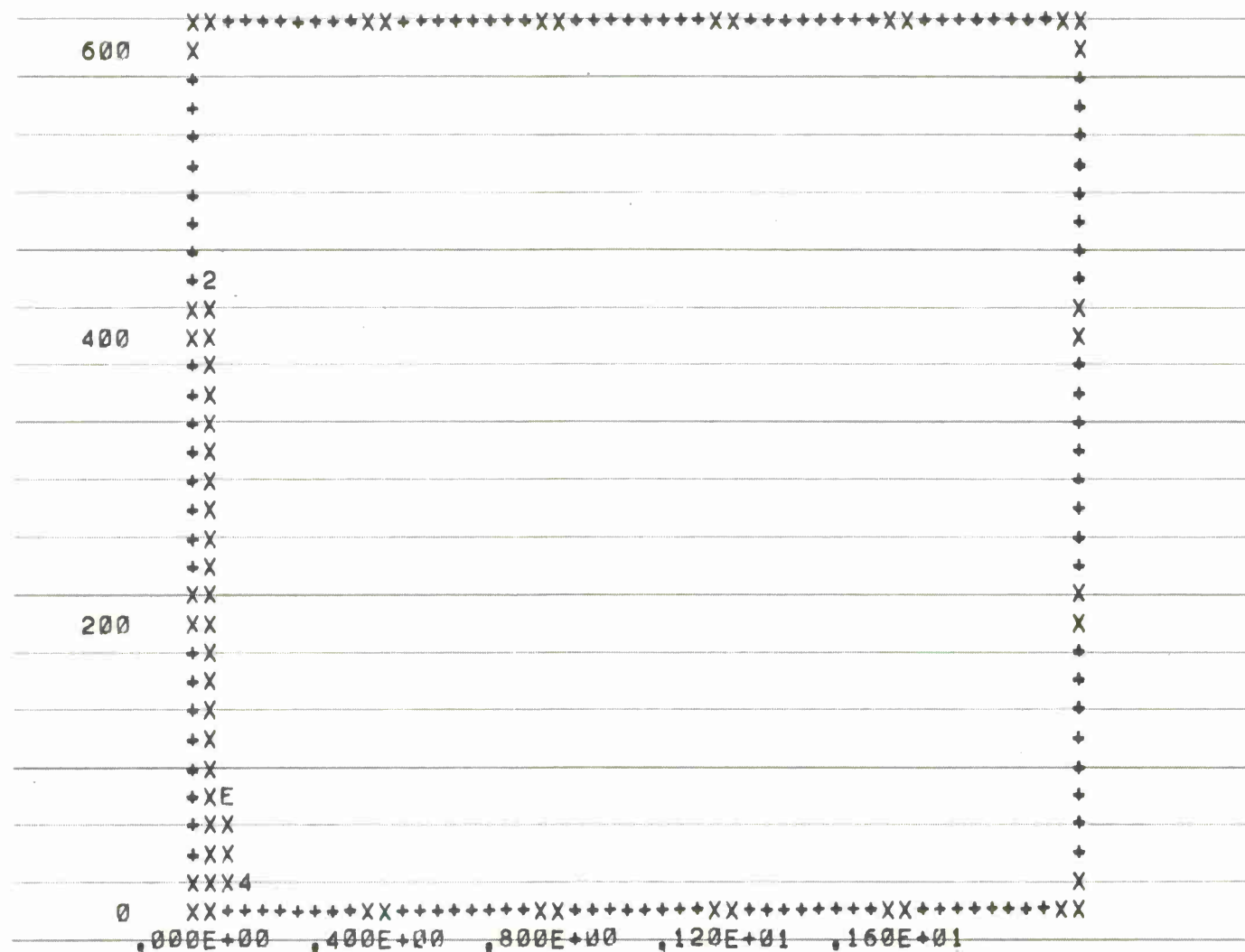
FIGURE 15   OUTPUT STATISTICS OF 19 ELEMENT FILTER WITH PRF OF 5.33 Khz, CLUTTER ONLY

FIGURE 16 OUTPUT STATISTICS OF 19 ELEMENT FILTER WITH PRF OF 5.33 Khz, TARGET PLUS CLUTTER

FIGURE 17 OUTPUT STATISTICS OF 23 ELEMENT FILTER WITH PRF OF 5.33Khz, CLUTTER ONLY

```
      XX++++++++XX++++++++XX++++++++XX++++++++XX++++++++XX
  400 X                                                  X
      +                                                  +
      +                                                  +
      +                       E                          +
      +                       X                          +
      +                       X                          +
      +                       X                          +
      +                       X                          +
      X                       X                          X
  200 X                       X                          X
      +                       X                          +
      +                       X                          +
      +                       X                          +
      +                       X                          +
      +                     2X1                          +
      +                     XXX                          +
      +                     XXX                          +
      +                     XXX                          +
      X                   1XXX1                1         X
    0 XX++++++++XX++++++++XX++++++++XX++++++++XX++++++++XX
     ,000E+00   ,400E+00   ,800E+00   ,120E+01   ,160E+01
```
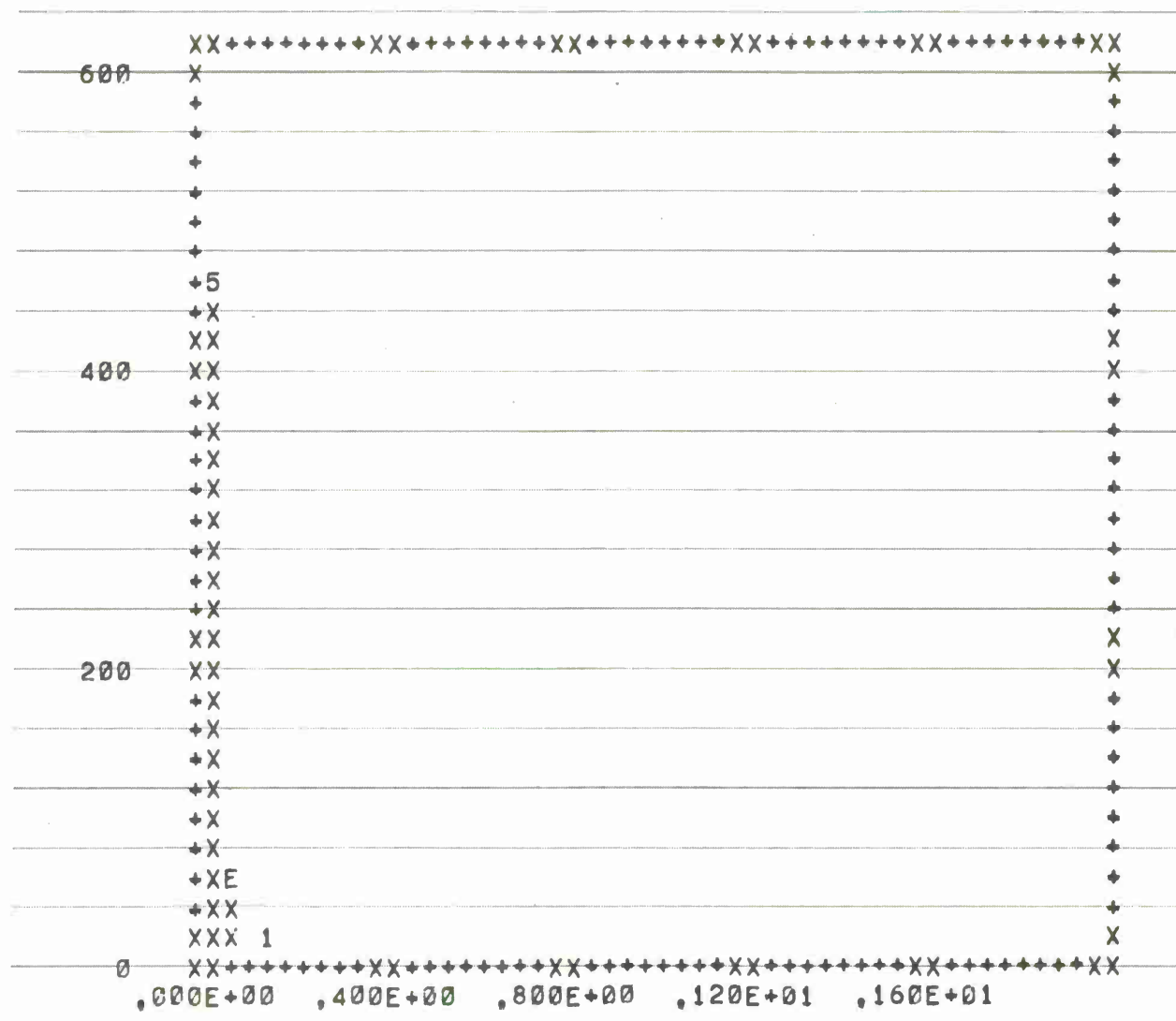
UNDERFLOW =   0   TOTAL =   500   OVERFLOW =   0
     AVERAGE =   .941   STANDARD DEVIATION =   ,037
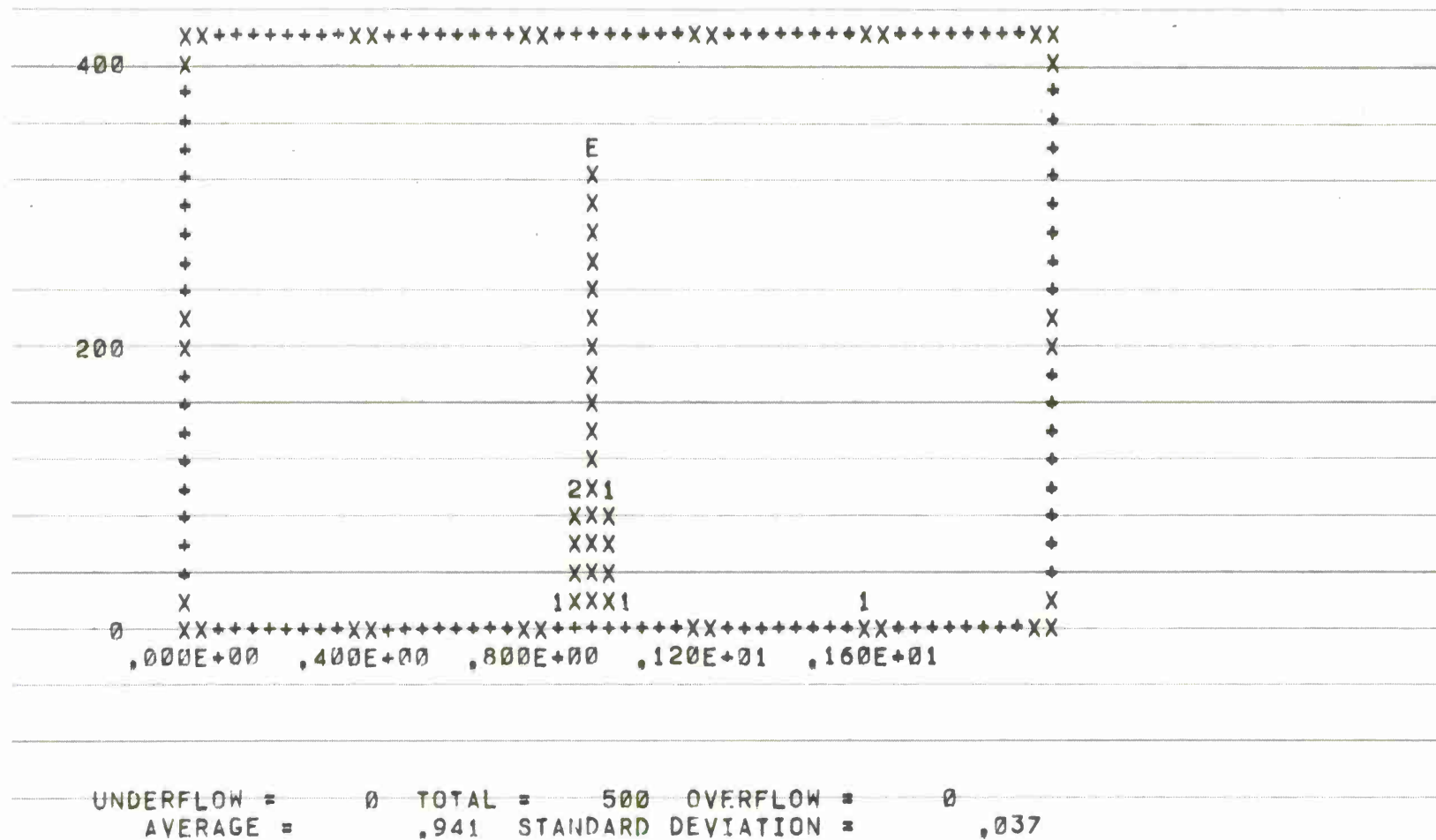
Each E Represents 14
Each X Represents 20

FIGURE 18   OUTPUT STATISTICS OF 23 ELEMENT FILTER WITH PRF OF 5.33Khz, TARGET PLUS CLUTTER

51

AUTOCORRELATION FUNCTION

$$\rho_{II}(\tau) = \frac{\Sigma I(t) I(t+\tau)}{\Sigma I(t) I(t)}$$

FROM NATHANSON et al.

$\lambda = 5.2$ cm

TIME (MILLISECONDS)
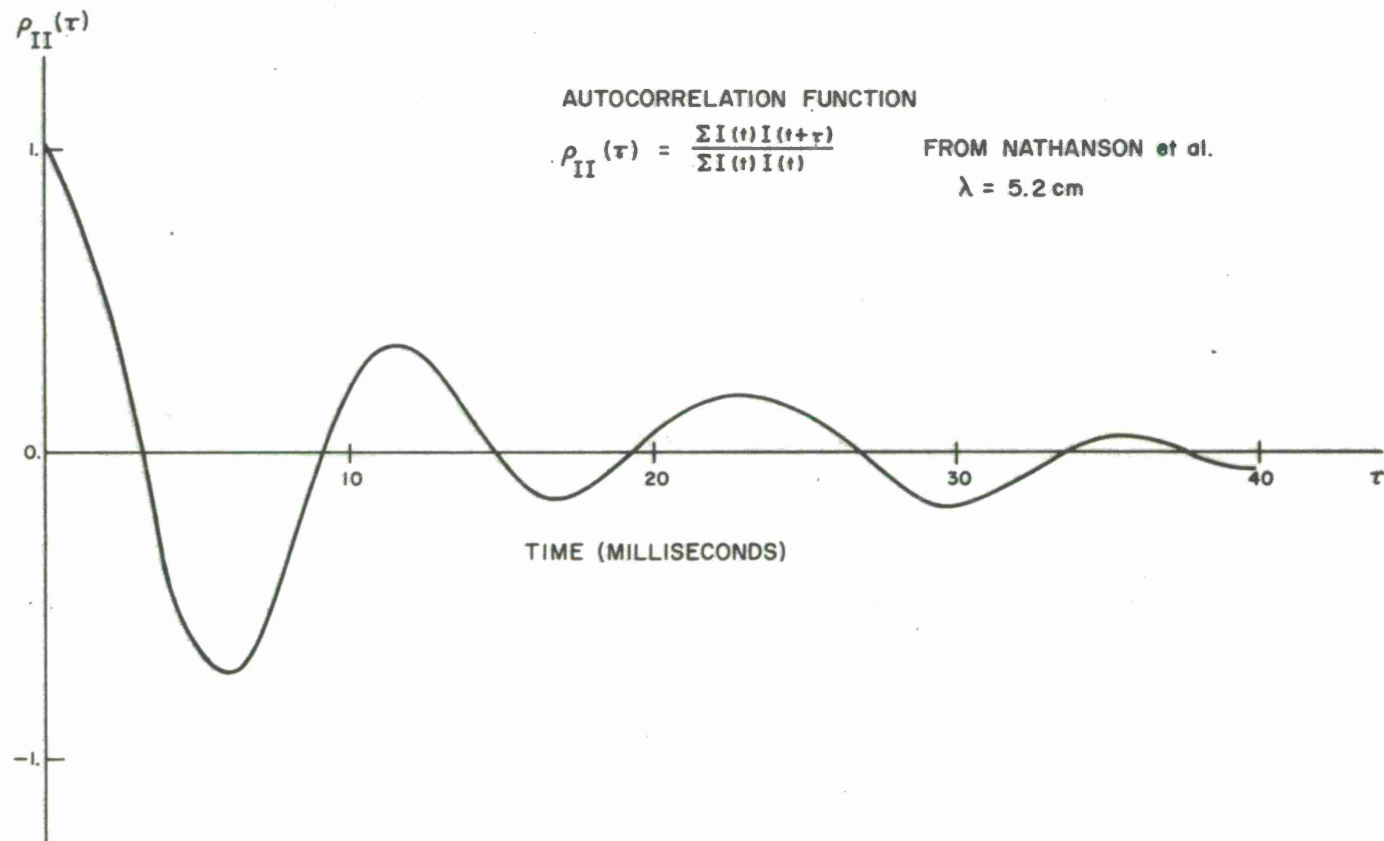
Figure 19   RAIN CLUTTER AUTOCORELLATION $\rho_{II}(\tau)$

52

$\rho(\tau)$

CORRELATION FUNCTION

$$\rho(\tau) = \sqrt{\rho_{II}^2(\tau) + \rho_{IQ}^2(\tau)}$$

FROM NATHANSON et al.
λ = 5.2 cm

1

0

10   20   30   40 τ

TIME (MILLISECONDS)
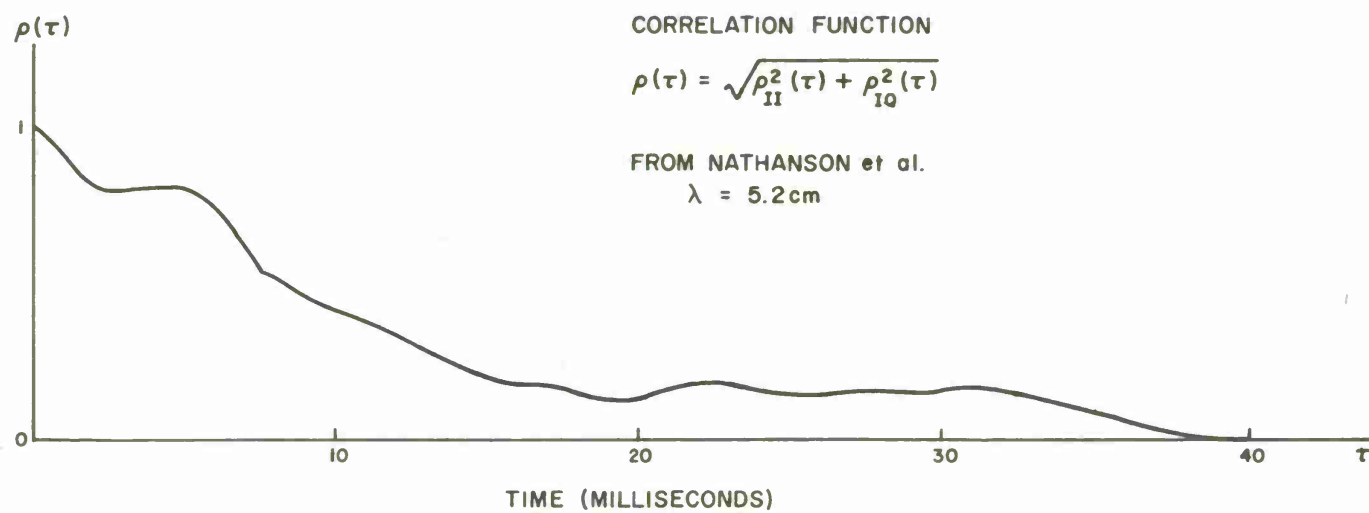
Figure 20   RAIN CLUTTER CORRELATION $\rho(\tau)$

APPENDIX A

RAIN CLUTTER SPECTRAL DISTRIBUTION

Consider a radar that has an illumination function defined as $I(\theta,\phi)$, such that

$$I(\theta,\phi) \, d\theta d\phi = 1 \tag{1}$$

Also, assume that ϕ and θ are independent and Gaussianly distributed.

$$\int \frac{d\theta e^{-\theta^2/2\sigma^2}}{\sqrt{2\pi} \, \sigma_\theta} \int \frac{d \, e^{-\phi^2/2\sigma^2}}{\sqrt{2\pi} \, \sigma_\phi} = 1 \tag{2}$$

If a radial velocity can now be formulated in terms of either or both of these angles, then the spectrum due to wind shear and beam broadening can be computed.

For wind shear, the velocity as a function of elevation height h is

$$V(h) = V_o + k \, h \, , \tag{3}$$

$$\nabla V = k \tag{4}$$

53

In the event that the elevation angle is small, then the height h can be related to the range and elevation angle as

$$h = R \sin\theta \approx R\theta \; , \tag{5}$$

$$= V_o + kR\theta \tag{6}$$

Assuming that the intensity pattern in the elevation angle is distributed as

$$p(\theta)d\theta = \frac{e^{-\frac{(\theta-\theta_o)^2}{2\sigma_\theta^2}}}{\sqrt{2\pi}\,\sigma_\theta} \tag{7}$$

then the average velocity and the standard deviation are

$$\langle v \rangle = \quad p(\theta)\,v(\theta)d\theta \tag{8}$$

$$\langle v \rangle = V_o + k\,R\,\theta_o \tag{9}$$

$$\sigma_v^2 = \langle(V-\langle v\rangle)^2 = k^2\,R^2\,\sigma_\theta^2 \tag{10}$$

$$\sigma_v = k\,R\,\sigma_\theta \tag{11}$$

54

The important feature of this result is that wind shear causes the Doppler velocity's spectrum width to increase linearly with range.

Beam broadening is the term that applies to wind driven clutter perpendicular to the bore sight.

Since the illumination pattern subtends other sectors than the boresight the radial velocity is

$$V_R(\phi) = V \sin \phi \qquad (12)$$

where V is the velocity of the wind perpendicular to the boresight

In the case of narrow gaussian beams

$$\langle V_R \rangle = 0 \qquad (13)$$

$$\sigma_v = V\sigma_\phi , \qquad (14)$$

or Beam Broadening is dependent linearly on the cross wind velocity.

Turbulence describes the statistical properties of the wind, and as such describes the variation of wind speed independent of height, range, etc. As such, it has been found that

$$\sigma_v^{TURB} \lesssim \cdot 7 \frac{m}{sec}^{[17,18]} \qquad (15)$$

55

Fall velocity contributes to the spectrum negligibly

$$\sigma_v^{vert} \sim \frac{1m}{sec} \tag{16}$$

Moreover for low elevation angles

$$\sigma_v = \sigma_v \, Sin\theta \sim \theta\sigma_v \ll \frac{1m}{sec} \tag{17}$$

which is entirely negligible.

Beam broadening for $\sigma_\phi = 1^o$ corresponds to $\sigma_v \sim \frac{1}{57} V$ cross wind.
If the cross wind velocity is $20 \, \frac{m}{sec}$, then for Beam Broadening

$$\sigma_v \sim \frac{.4m}{sec} \tag{18}$$

Shear constant $k = \nabla V$ has been found [17] to be approximately $5.7 \, \frac{m}{Sec \cdot Km}$
thus at a range of 10 km, and for a 1° Beam

$$\sigma_v^{Shear} = 10 \times \frac{5.7}{57} = \frac{1m}{sec} \tag{19}$$

It is not implausible to believe that these distribution widths
are independent, hence

$$\sigma_v^2 = \sigma_V^{2TURB} + \sigma_v^{2FALL} + \sigma_v^{2B.B} + \sigma_v^{2SHEAR} \tag{20}$$

APPENDIX B

FLUCTUATION CORRELATION

The autocorrelation functions denoted by $\rho_{II}(\tau)$, $\rho_{IQ}(\tau)$ and $\rho(\tau)$ are experimentally averaged with respect to time.

There are theorems[20] proved to state the ensemble averages equal averages with respect to time for stationary processes.

$$\lim_{T \to \infty} \frac{1}{2\pi} \int_{-T}^{+T} f(t) \ g(t+\tau)dt = < f(t) \ g(t+\tau) > \ , \tag{B1}$$

where the brackets denote a statistical average over the ensemble, and the time t is arbitrary, as are the function $f(\tau)$ and $g(\tau)$, with the provision that

$$<f(t_1) = <f(t_2)> \tag{B2}$$

$$<g(t_1) = <g(t_2)> \tag{B3}$$

as well as all the moments of f and g.

In the present case, the function

$$f(t) = \sum_{k=1}^{N} A_k \ \text{Cos} \ (\phi_k + \frac{4 \ V_k t}{\lambda}), \tag{B4}$$

57

$$g(t) = \sum_{k=1}^{N} A_k \, \cos \, (\phi_k + \frac{4\pi V_k t}{\lambda}) \tag{B5}$$

or

$$\sum_{k=1}^{N} A_k \, \sin \, (\phi_k + \frac{4\pi V_k t}{\lambda}) \tag{B6}$$

Define

$$\rho_{II}(\tau) \triangleq \frac{\int R_e \, R(t) \, R_e \, R(t + \tau) \, dt}{\int R_e \, R(t) \, R_e \, R(t) \, dt} \, , \tag{B7}$$

where R_e denotes real part,

$$\rho_{IQ}(\tau) \triangleq \frac{\int R_e \, R(t) \, Im \, R(t+\tau) \, dt}{\int R_e \, R(t) \, R_e \, R(t) \, dt} \, , \tag{B8}$$

where

$$R(t) = \sum_{K=1}^{N} A_k \, e^{j(\phi_k + \frac{4\pi V_k t}{\lambda})} \tag{B9}$$

describes the Ith and Q^{th} channel of the received signal from N scatterers at time t, each of which has an initial phase ϕ_k, and doppler velocity $\frac{4\pi V_k}{\lambda}$

Lemma I

For Gaussian velocity distributions

$$h(v)dv = \frac{e^{-\frac{(v-\bar{v})^2}{2\sigma_v^2}}}{\sqrt{2\pi}\ \sigma_v} \tag{B10}$$

$$\int R_e\ R(t)\ R(t+\tau)dt = \frac{N}{2}<A^2>\ e^{j\frac{4\pi\bar{V}\tau}{\lambda}}\ \bar{e}\ \frac{8\pi^2\tau^2\sigma_v^2}{\lambda^2}\ , \tag{B11}$$

then

$$\rho_{II}(\tau) = \cos\frac{4\pi\bar{V}\tau}{\lambda}\ \bar{e}\ \frac{8\pi^2\tau^2\sigma_v^2}{\lambda^2}\ , \tag{B12}$$

and

$$\rho_{IQ}(\tau) = \sin\frac{4\pi\bar{V}\tau}{\lambda}\ \bar{e}\ \frac{8\pi^2\tau^2\sigma_v^2}{\lambda^2} \tag{B13}$$

Thus

$$\rho(\tau) = \bar{e}\ \frac{8\pi^2\tau^2\sigma_v^2}{\lambda^2} \tag{B14}$$

Therefore,

$$\int R_e\ R(t)\ R(t+\tau)\ dt = <R_e\ R(t)R(t+\tau)> \tag{B15}$$

$$= \left\langle \left(\sum_{k=1}^{N}\ A_k\ \cos(\phi_k + \frac{4\pi V_k}{\lambda})\ \cdot\ \sum_{\ell=1}^{N}\ A_\ell\ e^{j\left(\phi_\ell + \frac{4\pi V_\ell}{\lambda}(t+\tau)\right)} \right) \right\rangle \tag{B16}$$

59

where the average is performed over A_k, ϕ_k and V_k .

Assuming that the drops are statistically independent, then making use of the following identities

$$\text{Cos } A \text{ Cos } B = \frac{1}{2} \left| \text{Cos } (A + B) + \text{Cos } (A - B) \right| \tag{B17}$$

$$\text{Cos } A \text{ Sin } B = \frac{1}{2} \left| \text{Sin } (A + B) + \text{Sin } (A - B) \right| \tag{B18}$$

and $\qquad\qquad <\cos \phi_k> \ = \ <\sin \phi_k> \ = 0, \text{ then} \tag{B19}$

with $\qquad\qquad A = \phi_k + \frac{4\pi V_k t}{\lambda} k \tag{B20}$

$$B = \phi_\ell + \frac{4\pi V}{\lambda} \ell \ (t+\tau) \tag{B21}$$

$$<\cos \ (\phi_k + \frac{4\pi V_k t}{\lambda})e^{j(\phi_\ell + \frac{4\pi V_\ell}{\lambda} \ (t+\tau)>} \ = \frac{1}{2} \ e^{j(\phi_k + \frac{4\pi V_k \tau}{\lambda})} \delta_{k\ell} \tag{B22}$$

whence the average over velocity and amplitude give

$$\int < R_e \ R(t) \ R(t + \tau)dt = \frac{N}{2} \ <A^2> \ < e^{j \ \frac{4}{\lambda} V \tau} > \tag{B23}$$

60

Finally, if Gaussian velocity distribution is assumed

$$<R_e \ R(t) \ R(t+\tau) = \frac{N}{2} \ <A^2> \ e^{j \ \frac{4\pi \bar{V} \tau}{\lambda}} \ \bar{e} \ \frac{8\pi^2 \tau^2 \sigma_v^2}{\lambda^2}$$ (B24)

Therefore

$$\rho_{II} \ (\tau) = Cos \ \frac{4\pi \bar{V} \tau}{\lambda} \ e^{-8\pi^2 \frac{\tau^2}{\lambda^2} \sigma_v^2}$$ (B25)

$$\rho_{IQ} \ (\tau) = Sin \ \frac{4\pi \bar{V} \tau}{\lambda} \ e^{-8\pi^2 \frac{\tau^2}{\lambda^2} \sigma_v^2}$$ (B26)

and

$$\rho \ (\tau) = \bar{e} \ \frac{8\pi^2 \tau^2}{\lambda^2} \sigma_v^2$$ (B27)

The power spectral density is also easily found to be

$$S(f) = \int e^{j2\pi f\tau} \int R \ (t) \ R^* \ (t + \tau) \ d\tau \quad ,$$ (B28)

but $$S(f) = \int e^{j2\pi f\tau} \ < R(\tau) \ R^* \ (t + \tau) > \ d\tau ,$$ (B29)

61

with $\quad < R(t)\, R^*(t+\tau) = <\left[\sum_k \left(A_k\, e^{j\phi_k} + \frac{4\pi V}{\lambda}kT\right)\right] \sum_\ell \left[A_\ell\, e^{-j\left(\phi_\ell - \frac{4\pi V}{\lambda}L(t+\tau)\right)}\right]>$

$$\text{(B30)}$$

$$= N <A^2> < e^{j\, 4\pi \frac{V}{\lambda}\tau} > \qquad\qquad \text{(B31)}$$

$$= N <A^2> > \bar{e}^{j\, 4\pi \frac{\bar{V}}{\lambda}\tau}\, e^{-8\pi^2\, \frac{\tau^2}{\lambda^2}\sigma_v^2} \qquad \text{(B32)}$$

where a Gaussian distribution for velocity is assumed.

Thus

$$S(f) = \int e^{j2\pi f\tau} < R(t)\, R^*(t+\tau) > d\tau \qquad \text{(B33)}$$

$$= \int e^{j2\pi f\tau}\, N <A^2>\, \bar{e}^{j4\pi\frac{\bar{V}}{\lambda}\tau}\, e^{-8\pi^2\, \frac{\tau}{\lambda^2}\sigma_v^2} \qquad \text{(B34)}$$

Noting that
$$\int e^{j\beta\tau}\, \bar{e}^{\tau^2/2\alpha^2} = \sqrt{2\pi}\ \alpha\ \bar{e}^{\frac{1}{2}\alpha^2\beta^2} \qquad \text{(B35)}$$

with $\qquad\qquad \alpha = \frac{\lambda}{4\pi\sigma_v}$ and $\beta = 2\pi f - \frac{4\pi\bar{V}}{\lambda}$, $\qquad \text{(B36)}$

then
$$S(f) = \frac{N <A^2>\, \sqrt{2\pi}\,\lambda}{4\pi\,\sigma_v}\ \bar{e}^{\frac{\lambda^2}{8\pi_v^2}\left(f - \frac{2\bar{V}}{\lambda}\right)^2} \qquad \text{(B37)}$$

62

APPENDIX C

Quantization Noise

In the process of performing analog to digital conversion of the Ith and Q^{th} channel, noise is introduced into the filtering process affecting the filter's performance.

In sampling the Ith and Q^{th} channel, if the time between successive samples is so rapid that, for a quantization level g, the autocorrelation function $\rho_{II}(\tau)$, (same for Q^{th} channel), cannot change appreciably in level, then systematic biases are introduced, i.e.,

$$1 - \rho_{II}(\tau) \lesssim g/2. \tag{C1}$$

We shall not consider this case, but rather the converse.

The text showed that half of the power is shared by the Ith and Q^{th} channel respectively. If each channel has M bits (1 bit for sign), and if the digitizer is to span $\nu\sigma$ deviation of the voltage spectrum of I and Q, then

$$g \cdot 2^{m-1} = \nu\sigma \tag{C2}$$

Straightforward probability arguments prove that if the signal populates the levels uniformly, with G, the true voltage in the quantum interval, then

$$<G> = 0 \tag{C3}$$

$$\sigma_G^2 = < (G - <G>)^2> \tag{C4}$$

63

$$= \frac{1}{12} g^2 \qquad\qquad (C5)$$

$$= \frac{\nu^2 \sigma^2}{12 \cdot 4^{m-1}} \qquad\qquad (C6)$$

In the case where clutter dominates the power spectrum

$$\sigma^2 = 1/2 \sum_k |A_k|^2 \qquad\qquad (C7)$$

(the factor 1/2, as the power divides between I and Q)

If $1 - \rho_{II}(\tau) \gtrsim g/2$ then the sampling will be independent, and the noise spectrum white.

The fraction of white noise due to sampling passed by the digital filter is now

$$\frac{2 \int <G^2> |F(w)|^2 \, dw}{\int dw} \qquad\qquad (C8)$$

For the digital filters in this study

$$\frac{\int |F(w)|^2 \, dw}{\int dw} \quad \stackrel{\sim}{=} \quad \begin{cases} \dfrac{2}{3} & @ \ 8.0 \ \text{KHz} \\[2ex] \dfrac{1}{2} & @ \ 5.33 \ \text{KHz.} \end{cases} \qquad (C9)$$

64

Thus, an upper limit can be placed upon the amount of noise due to quantization passed through the filters; it is

$$2 \; <G^2> \left\{ \begin{matrix} \frac{2}{3} \\ \frac{1}{2} \end{matrix} \right\} \; \gtrsim \; <G^2> \tag{C10}$$

$$= \frac{1}{12} \; \frac{\nu^2 \; \sigma^2}{4^{m-1}} \tag{C11}$$

For clutter with

$$\sigma^2 = \frac{1}{2} \; \Sigma \left| A_k \right|^2 \tag{C12}$$

$$= 50,$$

$\nu = 3$ standard deviation, and a 6 bit converter, the power passed is

$$\frac{3^2 . 50}{12 . 4^5} \; \gtrsim \; .075 \tag{C13}$$

Thus, the ratio of quantized noise to power in either the I $^{\text{th}}$ or Q$^{\text{th}}$ channel is

$$\frac{.075}{50} = .0015, \text{ or } 28 \text{ dB} \tag{C14}$$

For an 8 bit converter, the ratio is 40.0 dB.

REFERENCES

1. W.M. Bridge, "Measurements of the Depolarizing Effect of Rain on X-Band Propagation", MTR-2853, 1 July 1974

2. M.R. Weiss, "An Analysis of a Slotted Waveguide, Frequency Scanned, Antenna Near Cutoff",ESD-TR-74-197, DECEMBER 1974

3. Cook, C., Kramer, J.D., Smith, I., Yoder, L.W., "MITRE Recommendations for an X-Band Precision Approach Radar" MITRE Corporation, Bedford, Ma. , January 1973.

4. Gold, B., Rader, C., "Digital Processing of Signals" McGraw-Hill, New York, 1969.

5. Rabiner, L. Couley, J., Helms, H., Jackson, L., Kaiser, J., Rader, C., Schafer, R., Steiglitz, K., Weinstein, C., "Terminology in Digital Signal Processing," IEEE Audio and Electronics AU-20, No.5,322, Dec. 1972

6. Morse, P., Feshback, H., "Methods of Theoretical Physics," Vol. I, McGraw-Hill, New York, 1953.

7. Rabiner, L., "Approximate Design Relationship for Low Pass FIR Digital Filters", IEEE Trans. Audio and Electronics AU-21, No. 5, 456, October 1973.

8. Parks, T., McClellan, J., "A Program for the Design of Linear Phase Finite Impulse Response Digital Filters," IEEE Audio and Electronics AU-20, No. 3, 195, Aug. 1972.

9. Parks, T., "Chebyshev Approximation for Non-Recursive Digital Filters with Linear Phase", IEEE Circuit Theory, CT-19, No. 2, 189, March 1972.

10. Parks, T., Rabiner, L., McClellan, J., "On the Transition Width of Finite Impulse Response Digital Filters,"IEEE Audio and Electronics, AU-21, No.1, February 1973.

11. Rabiner, L., "Techniques for Designing Finite Duration Impulse Response Digital Filters", IEEE Trans. Communications Technology, COM-19, 188, April 1971.

12. Herrmann, O. "Design of Non-Recursive Digital Filters with Linear Phase", Electronics Letters, Vol. 6, May 1970.

13. Born, M, Wolf, E., "Principles of Optics," p.633 ff.,
    Pergamon Press, Oxford, 1963.

14. Gunn, K., East, T., "Microwave Properties of Precipitation
    Particles", Quarterly Journal of the Royal Meterological
    Society, 80:522, 1945.

15. Breuer, L.S., "Simultaneous Quantitative Measurement of Rainfall
    Rate and Drop Size Distribution", p. 167 of 15th Radar
    Meteorological Conference at Champaign-Urbanna, Illinois,
    October 1972.

16. Marshall, J., Palmer, W., "Distribution of Rain Drop Sizes"
    Journal of Meteorology, Vol. 4, 186, 1948.

17. Nathanson, F., Reilly, J., "Radar Precipitation Echoes",
    IEEE Aerospace and Electronics, AES-4, No. 4, 505, July 1968.

18. Battan, L., "Radar Observation of the Atmosphere", University
    of Chicago Press, Chicago, 1959.

19. Roberts, J., "Computation of P_D for the AN/TPN-19 PAR",
    ESD-TR-69-443, February 1970.

20. Khinchin, A. "Mathematical Foundations of Statistical Mechanics"
    p. 20 ff., Dover Publications, New York 1949.